Flight feather aerodynamics and its dependence on morphology and material properties

FRIDA ALENIUS
DEPARTMENT OF BIOLOGY | FACULTY OF SCIENCE | LUND UNIVERSITY

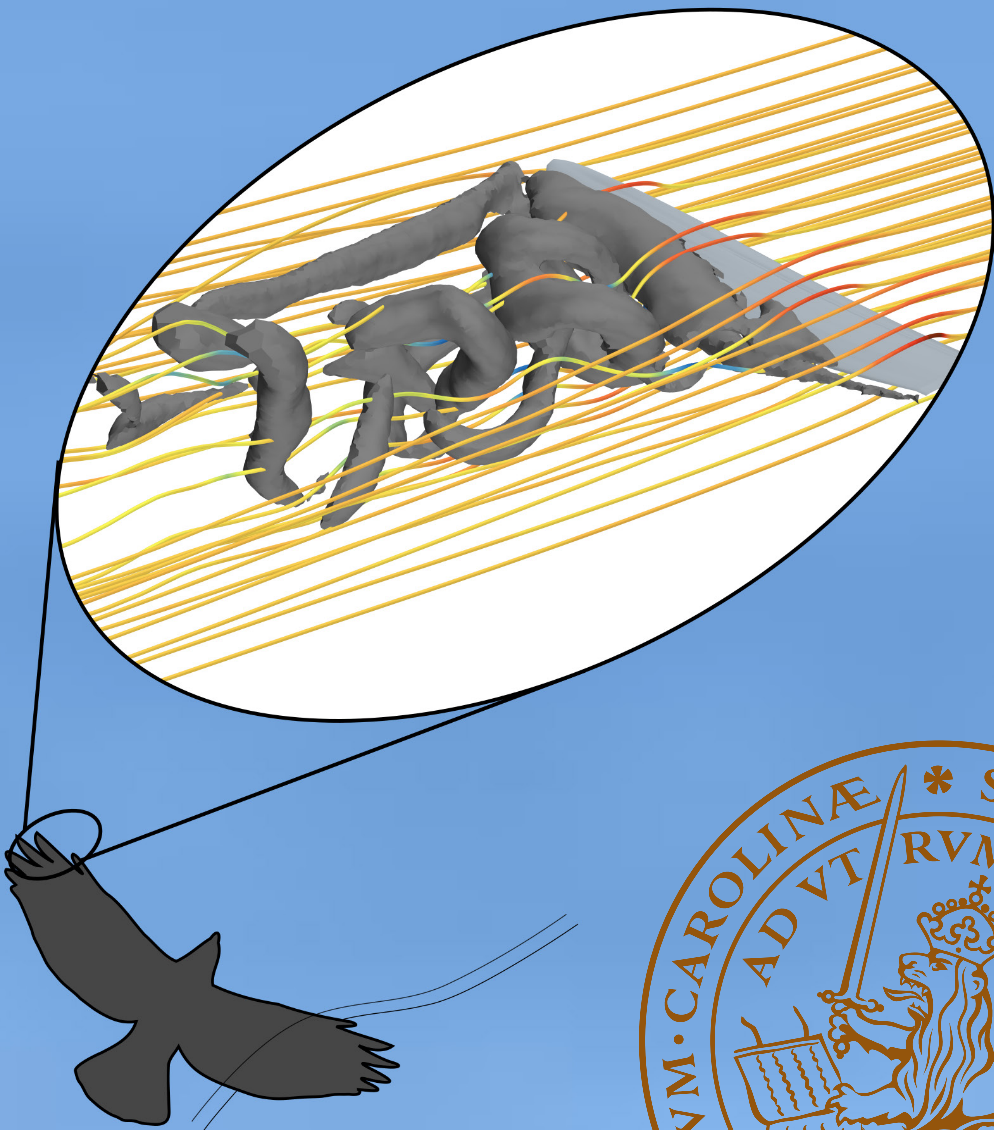

Flight feather aerodynamics and its dependence on morphology and material properties

PAPER 1

Alenius, F., Revstedt, J., Johansson, L.C., (2026). Feather aerodynamics suggest importance of lift and flow predictability over drag minimization. Sci Rep 16, 8380. https://doi.org/10.1038/s41598-026-41064-7

PAPER 2

Alenius, F., Revstedt, J., Johansson, L.C., Aerodynamic performance suggests shape of flight-feather microstructures is consistent with optimization. *Submitted*

PAPER 3

Alenius, F., Persson, K., Johansson, L.C., Revstedt, J., Flight feather performance is affected by material properties *Manuscript*

PAPER 4

Alenius, F., Revstedt, J., Persson, K., Johansson, L.C., Aeroelastic response to flight feather untwisting. *Manuscript.*

Printed by Media-Tryck, Lund 2026 NORDIC SWAN ECOLABEL 3041 0903

Faculty of Science
Department of Biology

LUND UNIVERSITY

ISBN 978-91-90202-49-4

Flight feather aerodynamics and its dependence on morphology and material properties

Flight feather aerodynamics and its dependence on morphology and material properties

Frida Alenius

DOCTORAL DISSERTATION

Doctoral dissertation for the degree of Doctor of Philosophy (PhD) at the Faculty of Science, Lund University. To be publicly defended on Friday October 2nd, 09.00 in Blue Hall, Department of Biology, Ecology building, Kontaktvägen 10, 223 62 Lund, Sweden.

Faculty opponent
Toshiyuki Nakata, PhD
Associate Professor, Graduate School of Engineering, Chiba University

Organization: LUND UNIVERSITY

Document name: Doctoral dissertation **Date of issue 2026-08-17**

Author(s): Frida Alenius

Title and subtitle: Flight feather aerodynamics and its dependence on morphology and material properties

Abstract:
For some bird species the outermost part of the wings, the feathers can separate from each other and the wing, in such cases each feather must act as an independent aerodynamic unit. In addition to regular function of flight feathers such as colouring and overall aerodynamic and structural capabilities, these separated feathers must withstand the aeroelastic demands on their own using the complex surface the microstructures of the feather create. It is known from the fossil record that the feather microstructures have evolved over time and that the modern flight feathers differ from the first birds. This thesis is a first step into exploring the behaviour of a feather and the impact on the air flow from its microstructures, using computational models. The computational models were based on a Jackdaw (Corvus monedula) ninth primary flight feather.

First, two papers examine the aerodynamics of a profile of a feather section and focuses on how profile shape and microstructures of the feather impact aerodynamic performance, using both the layout of microstructures found in Jackdaw today, as well as modified ones. Modifications are done by changing the microstructures relation to each other. Second, two papers examining the fluid-structure interaction effects of the entire outermost part of the feather. Material properties and overall shape is under consideration by tracking the general behaviour of the aeroelastic response.

The findings from the first two papers indicate that the feather profile in its current configuration operates at a local aerodynamic performance maximum. However, there are indications that flow predictability and shaft structural integrity is prioritized before aerodynamic efficiency. Suggesting that a trade-off between differing selection pressures (aerodynamic efficiency, aerodynamic stability and structural integrity) and developmental constraints exists. The findings of the third paper suggest that bend and angle of attack is governed by the material and structural properties, whilst the backwards sweep is also dependent on the relative movement of the barb and barbules. In the fourth paper the inherent twist of the feather does seem to have an aerodynamic advantage, and further studies are needed to fully understand its function.

In summary, the aim of this thesis was to take a first step to better understand feather behaviour in an air stream. The results suggest that trade-off between aerodynamic and structural function have been made and that more studies are needed to fully understand the complex nature of the feather. The results in this thesis could also be of interest when constructing low Re wings, especially those with highly flexible blades.

Key words: Feather evolution, Computational fluid dynamics, Fluid- structural interaction, Bio-inspired, Functional morphology, Flow stability, Avian biomechanics

Language: English **Number of pages**:72

ISBN (print): 978-91-90202-49-4 **ISBN (electronic):** 978-91-90202-50-0

Signature Date 2026-08-17

Flight feather aerodynamics and its dependence on morphology and material properties

Frida Alenius

Faculty of Science

Department of Biology

ISBN 978-91-90202-49-4 (print)

ISBN 978-91-90202-50-0 (electronic)

Printed in Sweden by Media-Tryck, Lund University, Lund, 2026

NORDIC SWAN ECOLABEL
Printed matter 3041 0903

Media-Tryck is a Nordic Swan Ecolabel certified provider of printed material. Read more about our environmental work at www.mediatryck.lu.se

MADE IN SWEDEN

Table of Contents

1.1. Abstract

For some bird species the outermost part of the wings, the feathers can separate from each other and the wing, in such cases each feather must act as an independent aerodynamic unit. In addition to regular function of flight feathers such as colouring and overall aerodynamic and structural capabilities, these separated feathers must withstand the aeroelastic demands on their own using the complex surface the microstructures of the feather create. It is known from the fossil record that the feather microstructures have evolved over time and that the modern flight feathers differ from the first birds. This thesis is a first step into exploring the behaviour of a feather and the impact on the air flow from its microstructures, using computational models. The computational models were based on a Jackdaw (*Corvus monedula*) ninth primary flight feather.

First, two papers examine the aerodynamics of a profile of a feather section and focuses on how profile shape and microstructures of the feather impact aerodynamic performance, using both the layout of microstructures found in Jackdaw today, as well as modified ones. Modifications are done by changing the microstructures relation to each other. Second, two papers examining the fluid-structure interaction effects of the entire outermost part of the feather. Material properties and overall shape is under consideration by tracking the general behaviour of the aeroelastic response.

The findings from the first two papers indicate that the feather profile in its current configuration operates at a local aerodynamic performance maximum. However, there are indications that flow predictability and shaft structural integrity is prioritized before aerodynamic efficiency. Suggesting that a trade-off between differing selection pressures (aerodynamic efficiency, aerodynamic stability and structural integrity) and developmental constraints exists. The findings of the third paper suggest that bend and angle of attack is governed by the material and structural properties, whilst the backwards sweep is also dependent on the relative movement of the barb and barbules. In the fourth paper the inherent twist of the feather does seem to have an aerodynamic advantage, and further studies are needed to fully understand its function.

In summary, the aim of this thesis was to take a first step to better understand feather behaviour in an air stream. The results suggest that trade-off between aerodynamic and structural function have been made and that more studies are needed to fully understand the complex nature of the feather. The results in this thesis could also be of interest when constructing low Re wings, especially those with highly flexible blades.

1.2. Popular science summary

Birds use their wings to fly, in some species, such as birds of prey and crows, the feathers on the outmost part of the wing slit apart and spread from the wing tip, to be on their own. This is called a slotted wing. The feathers in the slotted wing are not supported by any other feathers, and the demands they are subjected to is different than to feathers that have neighbours. This thesis explores the properties of a Jackdaws (*Corvus monedula*) ninth primary flight feather, including the material setup, how the air flow behaves around it and how the feather behaves itself. The ninth primary feather sits at the front of the wing at the most forward position in a slotted wing. The slotted feathers are very flexible, they can bend, sweep and rotate, and they appear to adjust its shape to the conditions around it. Feathers are made of keratin and when fully grown, are a dead structure. A single feather is not actively controllable by the bird, so any movement is governed by passive mechanisms. The size of a flight feather and its inherent components, shaft, barbs and barbules, make it difficult to create physical models. Therefore, computational models have been created to execute the work in this thesis. This thesis is divided into two main parts, the first part a model of a smaller section of the feather has been created, to study the detailed flow conditions around the feather. Second, a larger model consisting of the outer half of the feather where the interaction between the feathers movement and the airflow can be explored.

In the smaller model a detailed description of the flow around a part of the feather and the feather components have been done. Here the details of the feather components have been kept, something that is computationally costly due to the increased complexity of the model. However, this is a key factor to explore how each component interacts with the air around the feather. We made a CT scan of a Jackdaws flight feather. In **paper 1** we made a small, detailed model of a section of the feather that imitates the layout of the feather, as close as possible. In **paper 2**, the same model was used, however the relationship between the different component was changed to be able to explore the effect of the feather morphology in the airflow. Both **paper 1** and **paper 2** suggests that the shaft, especially the part on the ventral side of the feather have a negative effect on the aerodynamic properties. Given that it is still shaped like it is, is an indication that the shaft has other utilities for the feather, one such utility is the structural integrity, which is also suggested by the square shape that improves stiffness. Other modifications, changing the barb angle or barbule hight location, overall show less aerodynamic effectiveness, than the non-modified version. Suggesting that the current body plan of the feather, is as aerodynamically favourable as is possible with the constraints a feather is under. Such constraints include developmental constraint and the subparts a feather consists of, conflicting selection pressure from the structural demands or other less straight forward properties as ware resistance.

In the second model, a more simplified model than for **paper 1** and **paper 2**, larger part of the feather than the previous model was explored. This model covered the part of the feather that is located in the unsupported slotted wing position. To be able to investigate the interaction between the flow and the behaviour of the feather, a computational methodology called fluid- structure interaction (FSI) model was used. In these types of models both the airflow around the father as well as the feather's reaction can be explored. This is crucial in a model where the object is highly dynamic and changes shape depending on the surrounding input, just a feather does. In **paper 3**, the feather's different behaviours and robustness of behaviour, depending on the material properties was explored. The variables tracked was the upwards bend, the backwards sweep and the pitch angle of the feathers. In the simulations it was found that the upwards bend and pitch angle could be influenced by several different material parameters on both the vane and the shaft, whilst the backwards sweep was only affected by one variable on the vane. The fact that the upwards bend is affected by several variables indicates that the material properties of the feather has be explored further, to figure out the balance between the shaft and vanes in the performance of the feather. Especially if a larger system with several feathers is to be investigated. Additionally, the way the feather model responded to the backwards sweep suggests that the backwards motion is not only directed by the material properties but also from by the relative movements of the feather parts.

In the last paper, **paper 4**, the behaviour of the feather was investigated by changing the morphology, by stepwise removing the inherent twist of the feather. For the modifications of the with more twist we expected a passive detwist, however this was not the case. We found that the feathers behaviour was stable and predictable. However, the reason for the inherent twist remains unknown.

This thesis helps improve our basic understanding of how and why a feather behaves the way it does in the air. It offers a perspective on how the various subparts of a flight feather work together and interact with the airflow around it. More specifically, it provides a detailed look at the airflow around a section of the feather and examines how different feather components influence that airflow. Additionally, it explores how material properties affect feather behaviour and investigates how feather shape and structure contribute to its overall performance. Further studies are needed to fully understand the behaviour of the feather and the effect the subparts and morphology have on the aerodynamic efficiency and the effective shape. The results in this thesis could also be of interest when constructing low Re wings, especially those with highly flexible blades.

1.3. Populärvetenskaplig sammanfattning

Fåglar använder sina vingar för att flyga. Hos vissa arter, som till exempel rovfåglar och kråkfåglar, kan fjädrarna längs ut på vingarna frigöra sig från sina grannar och fungera som självständiga enheter. Fjädrarna i de här positionerna stöds endas av sina närmsta grannar i basen av fjädern, vilket också ställer andra krav på dessa fjädrar än andra typer av fjädrar. I den här avhandlingen undersöks egenskaperna i den nionde handpennan hos en Kaja (*Corvus Monedula*), vilket inkluderar materialegenskaper, hur luftflödet beter sig runt fjädern och även hur själva fjädern beter sig i ett luftflöde. Fjädrar längst ut på Kajans vinge är mycket flexibel, den kan böjas uppåt, svepas bakåt och rotera och till synes ändra form för att anpassa sig till luftflödet runt den. Fjädrar är gjorda av keratin och när de är fullt utvuxna är de döda strukturer som fågeln inte kan kontrollera med direkta medel. Storleken på en hanpenna och de delar som den är uppbyggd, skaftet, fanstrålar och bifanstrålar gör att de är svåra att bygga modeller av, de är mycket små. Därför så har jag valt att använda beräkningsmodeller för mina undersökningar. Den här avhandlingen är uppdelad i två olika delar, i den första delen har en mindre modell konstruerats av en del av fjädern för att studera beteendet i detalj. I den andra delen, en större modell av den yttersta delen av fjäder, där interaktionen mellan fjäderns rörelse och luftströmmen kan undersökas.

I den mindre modellen, med den mer detaljerade utformningen, så har flödet runt fjädersektionen och fjäderns komponenter undersökts. Att behålla alla dessa små detaljer är beräkningsmässigt kostsamt eftersom modellen blir mer komplex. Med det sagt så är nivån av detaljer nödvändigt för att man ska kunna förstå hur de påverkar flödet runt fjädern. Underlaget för modellerna var en CT scan av Kajans hanpenna.

I **paper 1** gjordes en noggrann undersökning av flödet och i **paper 2**, användes samma modell och relationen mellan de olika komponenterna undersöktes för att se vad fjäderns morfologi hade för påverkan på flödet. Både **paper 1** och **paper 2** visar att skaftet, speciellt på den undre sidan, har en negativ effekt på de aerodynamiska egenskaperna. Eftersom skaftet ändå ser ut som det för, indikerar att andra egenskaper än de aerodynamiska är den funktionen som har haft högst prioritet, till exempel så kan strukturell stabilitet ha haft en viktigare roll. Andra förändringar i fjädern, så som bifanstrålarnas position och fanstrålarnas vinkel visade också på lägre aerodynamiska egenskaper än den omodifierade modellen. Det indikerar att det upplägget som fjädern har idag är den mest aerodynamiska fördelaktiga med de begränsningar som finns. Några av dessa begränsningar inkluderar utvecklingsmässiga begränsningar, de delar som fjädern består av, motsträviga selektionstryck eller andra funktioner som är mindre lätta att undersöka såsom slitstyrka.

I den andra lite större modellen så undersöktes en förenklad version av fjäder. Den här modellen var gjord för att matcha den delen av fjädern som delade sig från resten av vingen. För att undersöka interaktionen mellan flödet och fjäderns rörelse, byggdes en fluid-, strukturinteraktionsmodell (FSI. I dessa typer av modeller så kan både flödet runt fjädern samt hur fjäder rör sig i luftflödet studeras på en och samma gång. Att ha möjligheten att göra det är viktigt när man har en modell som ändrar form allt eftersom krafterna på ytan förändras, precis som det är för fjädern. I **paper 3** så undersöktes fjäderns ändrade beteende när materialparametrarna i modellen ändrades. De variabler som undersöktes var böjning uppåt, svepning bakåt och anfallsvinkeln. För simuleringsmodellen visade det sig att flera av materialparametrarna påverkade resultatet för böjning uppåt och anfallsvinkeln medan endast en kunde påverka bakåtsvepet nämnvärt. Det faktum att flera parametrar kunde påverka böjningen och anfallsvinkeln visar på att fler studier behövs för att säkerställa att balansen mellan de olika parametrarna är korrekt, speciellt om flera fjädrar ska undersökas samtidigt. Det sättet som fjädern betedde sig i förhållande till bakåtsvepet indikerar att det sättet materialet är uppbyggt påverkar fanets beteende men de relative rörelserna mellan fjäderns olika delar har också en betydelse.

I det sista artikeln, **paper 4**, fjäderns beteende som beror på dess morfologi studerades, genom att stegvis ta bort den vridning som fjädern har. Vi förvändande oss att se en passiv vridning av fjädern för de höga anfallsvinklarna, men så var inte fallet. Resultaten visade att fjäderns beteende var stabilt och förutsägbart, men anledningen till varför fjäder har en vridning är fortsatt oklart.

Denna avhandling bidrar till en förbättrad grundläggande förståelse av hur och varför en fjäder beter sig som den gör. Den ger ett perspektiv på hur de olika delarna av en handpenna samverkar med varandra och med det omgivande luftflödet. Mer specifikt ger den en detaljerad beskrivning av luftflödet runt en del av fjädern och undersöker hur olika fjäderkomponenter påverkar detta flöde. Dessutom studeras hur materialegenskaper påverkar fjäderns beteende samt hur fjäderns form och struktur bidrar till dess övergripande funktion. Ytterligare studier krävs för att fullt ut förstå fjäderns beteende och hur dess olika delar och morfologi påverkar den aerodynamiska effektiviteten och den effektiva formen. Resultaten från denna avhandling kan även vara av intresse vid utvecklingen av vingar i låga Reynolds-tal, särskilt sådana med mycket flexibla vingar.

1.4. List of papers

Paper 1

Alenius, F., Revstedt, J., Johansson, L.C., (2026). Feather aerodynamics suggest importance of lift and flow predictability over drag minimization. Sci Rep 16, 8380. https://doi.org/10.1038/s41598-026-41064-7

Paper 2

Alenius, F., Revstedt, J., Johansson, L.C., Aerodynamic performance suggests shape of flight-feather microstructures is consistent with optimization. *Submitted*

Paper 3

Alenius, F., Persson, K., Johansson, L.C., Revstedt, J., Flight feather performance is affected by material properties *Manuscript*

Paper 4

Alenius, F., Revstedt, J., Persson, K., Johansson, L.C., Aeroelastic response to flight feather untwisting. *Manuscript.*

1.5. Authors Contributions

Paper 1

All authors contributed to the design and methodology. Model creation, data collection and visualization FA. JR performed the solver study. Writing first draft FA. All authors contributed to review and editing.

Paper 2

All authors contributed to the design and methodology. Model creation, data collection and visualization FA. Writing first draft FA. All authors contributed to review and editing.

Paper 3

All authors contributed to the design and methodology. Model creation, data collection and visualization FA. Wind tunnel experimental setup and execution LCJ. Writing first draft FA. All authors contributed to review and editing.

Paper 4

All authors contributed to the design and methodology. Model creation, data collection and visualization FA. Writing first draft FA. All authors contributed to review and editing.

Authors

Frida Alenius (FA), Christoffer Johansson (LCJ), Kent Persson (KP), Johan Revstedt (JR)

1.6. Abbreviations

Re	Reynold number
CFD	Computational Fluid Dynamics
FSI	Fluid-Structure interaction
FEqA	Feather Equivalent Aerofoil
FM	Feather Model

1.7. Acknowledgement

I would like to thank Christoffer for proofreading this thesis. Your inputs and comments made this thesis a better one. The project received funding from Swedish Research Council grant no 2017-03890 and 2022-02850, support from eSSENCE grant 3.3. All computations were enabled by the Swedish National Infrastructure for Computing (SNIC) partially funded by the Swedish Research Council through grant agreement no. 2018-05973 and National Academic Infrastructure for Supercomputing in Sweden (NAISS), partially funded by the Swedish Research Council through grant agreement no. 2022-06725. Computations were performed at the HPC centres Aurora and Cosmos, provided by LUNARC, The Centre for Scientific and Technical Computing at Lund University. As well as Tetralith provided by NSC the National Supercomputer Centre at Linköping University. I am grateful to Arne Hegemann for providing jackdaws and Stephen Hall for providing the CT-scanning and to all the students that provided initial tests that helped decide what the final model should look like.

2. Introduction

Birds are all around us, their wings can carry the birds through the air by creating lift and thrust. Wings are built by partly overlapping feathers and for some species, the feather on the tip of the wings can split apart, and the feathers function as independent aerodynamic units (KleinHeerenbrink et al., 2017; R. Å. Norberg, 1985). This split in the wing tip is called slotted wings, figure 2.1, and are observed in different species of birds, for example in birds of prey and crows (D. Liu et al., 2021). This includes the Jackdaw (*Corvus monedula*), and the Jackdaw ninth primary flight feather is the study object of this thesis.

Figure 2.1. Slotted wings vs unslotted wings

a) A flying jackdaw with it wings in the slotted position. In pink the ninth primary flight feather and the base of the models.
b) A siluette of a Jackdaw if it would not be able to separate its feahter into a slotted configuration.

Feathers, as a collective, have multiple functions, including flight, insulation, coloration, sensory input and protection (Prum, 1999; Terrill & Shultz, 2023), to name a few. These functions are performed by different types of feathers, including, but not limited to, flight feathers, down feathers, contour feathers and bristles feathers. Flight feathers are the primary load-bearing feathers during flight (Terrill & Shultz, 2023) and must therefore be both aerodynamically efficient and structurally sound. Additionally, in the slotted position, feathers are flexible and can bend, sweep, and rotate (Oorschot et al., 2020), adapting to the flow around it, and feathers do this passively without active input from the bird.

Modern feathers are different from the feather of the earliest birds, furthermore, feathers evolved before flight (Foth et al., 2014; Prum, 1999; Xu et al., 2014) . With multiple functions combined into the flight feathers, is it possible that any one function has taken precedence over the others, or is the performance of the feather the results of a compromise? This thesis aims to increase the knowledge about the flow around a flight feather, the feathers response to the flow and why the feathers microstructures are configured as they are. To be able to achieve this, modifications of the feather and its microstructures, as it is known today, is necessary.

A Jackdaw is ~170 mm long and 14 mm wide, at the widest point, with individual structures in the <1 mm range (own measurements). The size of feathers, and especially the individual components are prohibitively small to be able to make reliable physical models to test in a wind tunnel. This is true both for a feather with the layout of the jackdaw feather but also for a model where the feather has been modified to examine the effect a modification has on the feather's behaviour. Another option is to make computer models, which is the main method of use in this thesis. Two types of models have been made, the first is a fluid dynamic computational (CFD) model and the second is a fluid-structure interaction (FSI) model. Both model types are used to understand the basic interaction between the flow of air and the feather, the feathers response to the air flow and how the feather components contribute to the feather's overall response to the air.

3. Aims

The goal of this thesis was to contribute to the understanding of flight feather behaviour and add more in-depth knowledge in an area to an area that have been little studied in great detail. Another goal was to explore if it was possible to uncover some of the evolutionary trade-offs that has led to the current morphology. This was done by using two different computational modelling methods, for the first two papers fluid dynamic models has been utilized and for the last two papers a fluid-structure interaction model, have been utilized.

For the first to papers the general aim was to gain a deeper knowledge about the flow around the feather and what effect the feather microstructures have on the performance of the feather. A detailed model of the current microstructure morphology was studied, as well as a model that could handle changes to the microstructure morphology.

For the last two papers the general aim was to further investigate the behaviour of the feather, using the entire outer part of the feather. Primarily, by exploring how the material properties influence the general behaviour and secondly how changing the inherent morphology of the feather impact behaviour and performance.

3.1. Paper specific Aims

3.1.1. Paper 1

The flow around a section of the flight feather located in the slotted wing tip was investigated. The aim was to describe, in-depth, how the air behaves around the feather and what impact the feather have on the flow, to understand the aerodynamic performance and potentially the responding behaviour of the feather. Additionally, a simplified model was created to better understand the general impact of the microstructures.

3.1.2. Paper 2

The effect of the feather morphology on the flow around the feather model was investigated. The aim was to describe the response the flow had to morphological changes of the feather microstructures, to see if some of these changes could explain why the current feather structure has been selected towards.

3.1.3. Paper 3

The flow around a feather model, representing the outer part of the feather, was studied to investigate the behaviour of the feather when material properties were changed. The aims were to find a setup that represents the feather's behaviour, gauge the general behaviour of the feather as well as the impact the material properties had on feather performance. If possible, also explain the robustness in performance seen in feathers.

3.1.4. Paper 4

The flow around a feather model, representing the outer part of the feather, was studied to investigate the behaviour of the feather when changing the overall inherent morphology in the feather and examine the response from the model. This was done by changing the built-in twist of the shaft, to explore the reason the feather has a built-in twist, and how this could relate to the passive control mechanisms suggest for these feathers.

4. Background

In this thesis I have built computer models of a bird's flight feather, with the goal to explore its morphology and behaviour. Therefore, an understanding of how a real feather is built is necessary. This includes the way the microstructures interact with each other, how each of the microstructures are internally structured as well as what material the microstructures are made of. Therefore, this chapter will explain how a feather is built, both what structures the feather is built out of, how those structures are structured and their in general response to their environment. Additionally, some basic understanding of aerodynamic and aeroelastic considerations must be made, to correctly setup the models.

4.1. Feather build

4.1.1. Feather components

A feather has a distinct shape, with the shaft in the middle and two vanes on either side (figure 4.1), which, depending on the type of feather, can be different sizes (Feo et al., 2015; Feo & Prum, 2014; Kiat & O'Connor, 2024). A flight feather, the type of feather used in this thesis, has a smaller anterior vane and a larger posterior vane (Feo et al., 2015; Kiat & O'Connor, 2024). The vanes are built from two components (Feo et al., 2015; Lucas & Stettenheim, 1972; Sullivan et al., 2019) (figure 4.1 c d). First, the barbs that branch out at an angle from the shaft, and second, the barbules that branch out, also at an angle, from both sides of a barb (Hendrickx-Rodriguez & Lentink, 2025; Lucas & Stettenheim, 1972). Barbs are stacked throughout the length of the shaft, and barbules from adjacent barbs hook together with a hook and groove system (Hendrickx-Rodriguez & Lentink, 2025; Lucas & Stettenheim, 1972), thus creating a sheet like structure that is referred to as the vane (figure 4.1 c d). There is a large differences in size between the components (Hendrickx-Rodriguez & Lentink, 2025; Lucas & Stettenheim, 1972; Sullivan et al., 2019) (figure 4.1), where the barbs do not have the same hight as the shaft for part of the feather. They are neither placed as high up as the shaft and it is only towards the distal tip of the feather where the top of the shaft and the top of the barbs are the same location. The discrepancy of the heights of the shaft and barbs, as well as how the barbs are stacked, make the dorsal and ventral surface of the feather non-smooth surfaces.

Additionally, the length and angle of the barb introduces a possibility of variation between different feather types and in a single feather (Feo et al., 2015). In flight feathers generally (Feo et al., 2015; X. Wang et al., 2019) and Jackdaw specifically, the anterior vane is narrower than the posterior vane, making the vanes asymmetric.

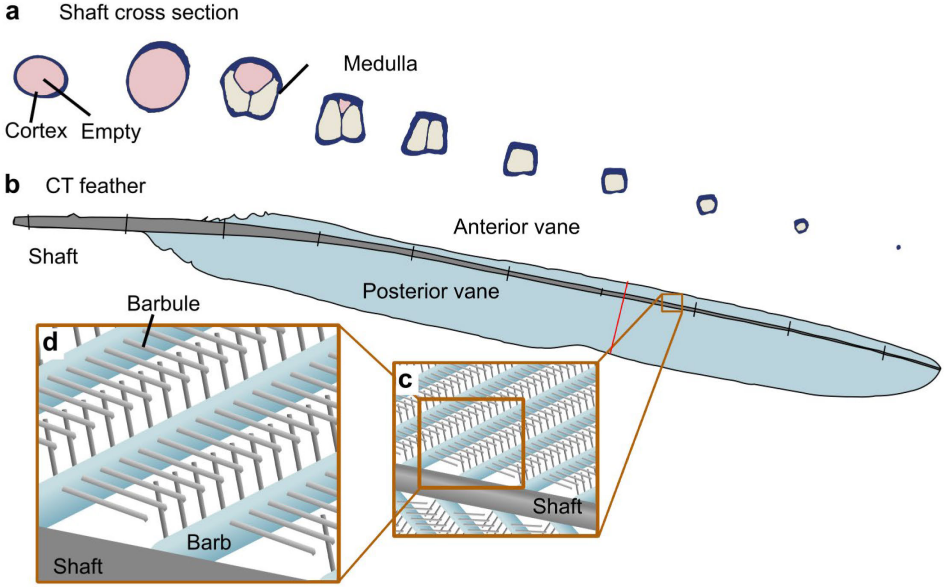

Figure 4.1. Feather geometry

a) Shaft cross section. The cross section of the shaft is changing throughout the length of the shaft, from the outer shape to the inner structures. At the base, the shaft is hollow with only the outer cortex to support it. As the shaft continuous, the medulla, a foam type substance fills the parts of the interior compartments until the medulla fills the entire inside. At the very tip of the shaft the entire core is solid.

b) An illustration of the top view of the CT scanned ninth primary flight feather of a Jackdaw.

c) A zoom in on the barb and barbules, the barbs stack closely together throughout the length of the shaft.

d) Additional zoom in on the barbs and barbules to showcase their overlapping nature. The top barbule has a hook where it hooks on to the bottom barbule from the adjacent barbule.

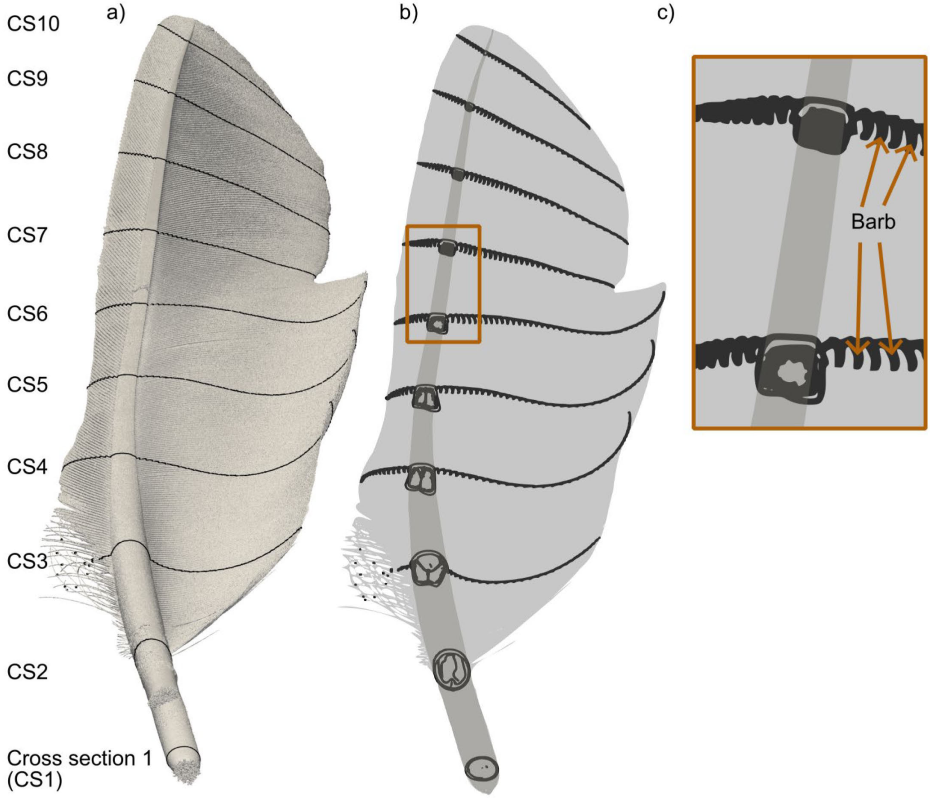

Figure 4.2. CT scanned feather with cross sections.
View of feather dorsal surface with several cross sections throughout the shaft, the location where the barbs attach to the shaft shift as well as how much of the hight of the shaft is matched by the barb hight throughout the length of the shaft. Also note the inherent twist of the shaft.

a) The dorsal side of the CT scanned Jackdaw feather, with cross sections marked.
b) Only cross section of the scanned feather, the relative hight of the barbs vs shaft increases throughout the length of the shaft.
c) Magnification of the cross section, marking some of the barbs, note the difference in barb hight vs the shaft height.

4.1.2. Feather shaft (cross section and fibre directions)

The shaft of a bird feather is divided into two parts; the calamus and the rachis (Lucas & Stettenheim, 1972). The calamus is the part that is embedded in the skin and the rachis is the part that the barbs branch out from (Hendrickx-Rodriguez & Lentink, 2025; Lucas & Stettenheim, 1972). The cross section of the shaft is not constant (Bachmann et al., 2012; Hendrickx-Rodriguez & Lentink, 2025; Schmitz et al., 2015), Figure 4.1 and Figure 4.2. At the base of the feather the cross section has an oval shape (CS1) with an empty core, as the shaft stretches on the oval shape continues but grows in diameter (CS2). As the barbs starts to branch (CS2), the ventral side of the shaft starts to square off and at the same time forming two internal compartments containing the medulla (CS3), a cellular material (W.-L. Chang et al., 2019; Hendrickx-Rodriguez & Lentink, 2025; Sullivan et al., 2017; Weiss & Kirchner, 2010), and a hollow part of the feather with its oval shape continues to shrink at the dorsal side of the shaft. The separation of the two compartments is called the transvers septum (Bachmann et al., 2012; Purslow & Vincent, n.d.), and the form of this wall can be different between species (W.-L. Chang et al., 2019). The two compartments grow along the shaft and first eliminate the hollow parts and at the same time the cross section forms a square rather than an oval (CS3-CS4). As the shaft stretches on the cross-section tapers (CS4-CS10), and the two compartments become a single compartment filled with the same medulla cellular material (CS5-CS9). At the very tip of the shaft the cross section again has a more circular shape, and the core is fully solid (CS10).

All components of the feather (shaft, barb and barbules) are made up of beta keratin (Greenwold et al., 2014; Hendrickx-Rodriguez & Lentink, 2025; Sawyer et al., 2000) and the keratin fibres are structured in fibre bundles (Lingham-Soliar, 2014). The fibre directions are not constant throughout the shaft; they run longitudinal (Lingham-Soliar, 2014; B. Wang & Meyers, 2017) in the part of the shaft that have a circular cross section as well as in the dorsal and ventral parts of the square cross section (figure 4.3). In the lateral parts (sides) of the square cross section, two set of keratin fibres are run at a 45° angle to the shaft i.e. 90° between the fibre sets (Lingham-Soliar, 2014; B. Wang & Meyers, 2017) (figure 4.3)). The keratin fibre alignments in the barbs are structured in same way as the shaft (Lingham-Soliar, 2014). However, the barbs have a more rectangular shape compared to the shaft circular/square shape. An internal compartment that is filled with a cellular medulla and an advantageous cross section for resisting bending, is also the way the barbs are built (Butler & Johnson, 2004; Hendrickx-Rodriguez & Lentink, 2025; Sullivan et al., 2016).

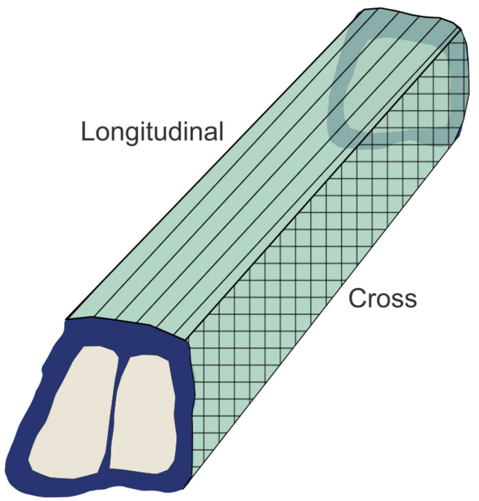

Figure 4.3. Illustration of the fibre directions in the shaft
Main fibre direction on top is longitudinal and on the side is criss cross. On the ends of the shaft section are cross section 5 and 6 (CS5 and CS6) displayed in Figure 4.2.

The longitudinal alignment of the keratin fibres on the top and bottom of the shaft allow them to flex, which govern the dorsal-ventral motion of the feather (B. Wang & Meyers, 2017). Whilst, the criss cross pattern, on the sides, increases the ability to sustain the attachment of the barbs to the shaft in this area (B. Wang & Meyers, 2017), compared to a longitudinal alignment (B. Wang & Meyers, 2017), as well as torsional rigidity (B. Wang & Meyers, 2017). For the entire shaft length, an outer layer of keratin fibres is laid in a circular direction, encasing all of the other fibres with their differing alignments (Lingham-Soliar, 2014; B. Wang & Meyers, 2017). All the layers in the feather are all made of the same material, keratin, glued together with a polymer interface (Lingham-Soliar, 2014). The way the material and the layering is setup can be compared to a laminate composite (Clyne & Hull, 2019), but contrary to most engineered composites, the layers in the feather are all made of the same material, keratin, glued together with a polymer interface (Lingham-Soliar, 2014). Comparing the feather to an engineered system that has an overall similar structure, long with high aspect ratio fastened in one end, such as a wind turbine (‘Introduction to Wind Turbine Blade Design’, 2023), the internal build is similar (figure 4.4). Although, the proportions and size are different, they both have an aerodynamic surface (red), main load baring structure (blue) and shear structure (neon blue). This with the origin being quite different, the feather has evolved over a long time and the wind turbine constructed by engineers.

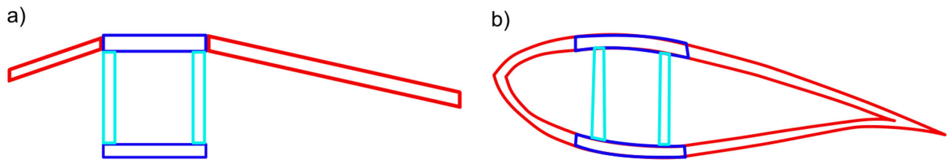

Figure 4.4. Feather outline vs turbine blade outline.
Blue spar cap, neon blue shear webs, red aerodynamic surfaces
a) Feather outline
b) Turbine outline

4.1.3. The feather material

The feather components are made up of one single type of material, the keratin fibres. However, the way it is laminated makes it necessary to investigate the material properties as it is found in the feather and not only the keratin itself if a proper computational model is to be built. The complex structure of a feather with its hierarchal build requires that the subparts (shaft, barbs and barbules) be separated to find the properties for each part. Previous studies have therefore focused on single elements of the feather, where the primary focus has been on the shaft due to its load bearing importance (B. Wang & Meyers, 2017). A general span of Youngs modulus (E), which describes the stiffness of a material, of 1-8 GPa (Bachmann et al., 2012; Bonser & Purslow, 1995; Cameron et al., 2003) can be found over a range of species, however, whether this value is constant over the entire length of the shaft depends on the study (Bachmann et al., 2012; B. Wang & Meyers, 2017). It is also debated how much the medulla and transverse septum contributes to the stiffness (Lingham-Soliar et al., 2009; Purslow & Vincent, n.d.) or have other main functions such as weight reduction. Another inherent property of the shaft is the second moment of area, which is calculated using the cross section of the shaft. This value is not constant over the feather length, due to the changing cross section and will vary greatly over the length of the shaft (Bachmann et al., 2012; Purslow & Vincent, n.d.). The barbs and barbules have also been studied, but to a lesser degree. Examples on studies include, the behaviour of the barb under load (Sullivan et al., 2016) or what happens when the barbules separate from each other (Ennos et al., 1995). Both studies, focuses on behaviour rather than material properties.

4.1.4. General movement of the feather

In a slotted wing (figure 2.1), the flight feathers spread apart creating slots between the wingtip feathers, the base of the feathers are supported by an adjacent feather while the outer part is not. The position where the flight feather goes from supported to unsupported is at the notch, the location on the vane where the width changes noticeably. The part of the feather that has no support from its neighbours must manage the forces exerted from the flow individually. Flight feathers show a great deal of flexibility in movement, they bend dorsally (Oorschot et al., 2020), sweeps backwards (Oorschot et al., 2020) and twist along the shaft (Oorschot et al., 2020). These movements can be large in multiple directions at once (Oorschot et al., 2020), where the feather structure in combination of the material properties must accommodate the movement. The feather barbs and barbules are constructed in such a way that they can move relative to each other without the barbules detaching (Ennos et al., 1995). Even though the barbules' hook system at first glance may seem to not allow any movement, it is possible for them to move (Ennos et al., 1995). The barbules from one barb can slide along the barbules from the adjecent barb, and the barbules can also bend, changing the angle to the barb and consequently the distance between the adjacent barbs (Ennos et al., 1995). Barbules and barbs are flexible and since they are only attached at the base, they have several degrees of freedom to move relative each other. All the movements described are passively done by the feather without direct control by the bird.

4.2. Moving through the air

In a flight feather, it is mainly the vanes that forms the surface the air flows around and interacts with. Even though the vanes are the main surface, the shaft contributes to the surface since it holds the two vanes together, additionally, it also transfers forces on the feather to the body of the bird. When flight feathers spreads out from the wing into the slotted configuration, they functions as an independent aerodynamic unit (KleinHeerenbrink et al., 2017; R. Å. Norberg, 1985). This means that the feather need to be able to maintain its shape, under different conditions such as wind gusts or flapping flight (KleinHeerenbrink et al., 2017).

4.2.1. Aerodynamics

The airflow around a flying object exerts forces on it (Gasiorek et al., 2006). A force perpendicular to the air flow is called the lift (Gasiorek et al., 2006). In addition to lift, a force parallel to the air flow is called the drag (Gasiorek et al., 2006) and is created as the flying object pushes through the flow. The drag force is directed opposite the flying direction and must be overcome by a thrust force propelling the aerofoil forward. In aerodynamics, an object that is created to generate more lift than drag is called an aerofoil (Gasiorek et al., 2006). Generally, an aerofoil is the surface of wing but in the case of this thesis it is the feather. Independent on what surface the air flows over, the underlying physics is complicated, and, the airflow can be both unsteady and non-uniform (Gasiorek et al., 2006), which can introduce three-dimensional phenomena (Gasiorek et al., 2006) . One way of characterizing the expected flow around an object is by the Reynolds number (Re), Eq 4.1.

$$Re = \frac{Inertial\,force}{Viscous\,force} = \frac{U_{\infty}c}{\nu} \qquad \text{Equation 4.1}$$

Where U_{∞} is the free stream velocity, c is the chord length and ν is the kinematic viscosity. The chord is defined as the distance between the leading edge and the trailing edge.

Aerofoils are streamlined and optimized for the intended use, for example the thickness and the camber, including optimal speed and propulsion type (Gasiorek et al., 2006). The flow phenomena interacting with the aerofoils are dependent on Re. When using the entire bird or bird wing as the reference the Re is in the range of 100,000 – 500,000 (Ajanic et al., 2023; KleinHeerenbrink et al., 2016; Lentink & Kat, 2014; U. M. Norberg, 1990; Pennycuick, 2008), however when analysing the stand alone feather, the chord is smaller. For the jackdaw feather used here the Re number is in the range of ~7000, where it is possible for the flow to be laminar (Gasiorek et al., 2006). At this low range of Re, the flow phenomena occurring for standard aerofoil and plates are, but not limited to, laminar separation bubble (Chen et al., 2013; Klose et al., 2021; Winslow et al., 2018), flow separation (Badrya et al., 2018; Chen et al., 2013; Klose et al., 2021; Winslow et al., 2018) and several modes of vortex shedding (Badrya et al., 2018; J. Chang et al., 2022; Klose et al., 2021; Spedding et al., 2008). Another variable that affects these phenomena is angle of attack, which is defined as the angle between the flow and the chord of the study object. The angle of attack will increase or decrease the likeliness of the flow phenomena to occur or how severe they are (J. Chang et al., 2022; Klose et al., 2021, 2025). For example, the higher the angle of attack, the more likely it is for the flow to separate and the flow to start shedding (J. Chang et al., 2022; Klose et al., 2025). During the shedding cycle the pressure distribution on the surface will change, leading to a change in lift and drag magnitude (J. Chang et al., 2022; Klose et al., 2025). The angle of attack of the feather can change for different reasons, gusts, flying mode (Klein Heerenbrink et al., 2015; R. Å. Norberg, 1985), or other voluntary moves, but also the built-in features of the feathers, such as a built-in twist, will subject the feather to different flow conditions.

In this thesis, the study object was a Jackdaw flight feather. Feathers in general have a complex surface, the individual components (shaft, barbs and barbules) make it so. Especially compared to a flat surface or an engineered aerofoil, which is often considered in aerodynamics, and very unlike how one would think about an aerofoil. The non-smooth surface created by the barbs and shaft effects the flow (van Bokhorst et al., 2015) and could influence the pressure distribution over the surface or where the flow separates (van Bokhorst et al., 2015). This in turn could affect the how aerodynamically efficient the feather is or how the flow interacts with feathers behind. As described earlier, the feather is also flexible and showcases an ability to bend, sweep and pitch with the shaft as an axis (Oorschot et al., 2020). In engineering, when a system interacts over the boundary of aerodynamics and solid dynamics it is called aeroelasticity (Dowell, 2022). The feather is a good example of an object that exhibit aeroelastic properties, placing it in the centre of three fields of study, biology, aerodynamics and structural dynamics. Understanding how and why the feather behaves like it does, opens the possibilities to mimic it and be able to utilize the multipurpose properties it possesses.

5. Methods

The small scale of the feathers make them difficult to extensively study, especially when intending to make morphological changes. The reason for this is that physical models are difficult to manufacture with high tolerances and wind tunnels setup and recording equipment may have to be run at the extremes of its capabilities. Therefore, the main method used in this thesis are computational models. For the first two papers (**paper 1** and **paper 2**) the main method to investigate the flow around the feather is a computational fluid dynamics (CFD) model. For the last two papers (**paper 3** and **paper 4**) fluid-structural interaction (FSI) models have been utilized. FSI is a combination of CFD and structural dynamics models, which makes it possible to investigate the entirety of the aeroelastic behaviour.

5.1. Computational Methods

5.1.1. Computational fluid dynamics

Computational fluid dynamics (CFD) is a method to solve fluid flow problems (Versteeg & Malalasekera, n.d.) and uses numerical algorithms to do so. Solving fluid flow problems is complex and flow behaviour is described by the properties of the flow specifically, velocity, pressure, density and temperature, and their space and time derivatives (Versteeg & Malalasekera, n.d.) (elements and time step). A fluid flow problem is based on the mathematical description of the conservation of mass, momentum and energy.

Mass conservation, Eq 5.1, states that the change rate of mass inside a fluid element is the same as the flow of mass into the fluid elements over its boundaries and is defined by the density ρ and the velocity vector u of the fluid (Versteeg & Malalasekera, n.d.). The conservation of momentum, Eq 5.2, is based on Newtons 2nd law and states that the change of momentum is equal to the sum of the forces on the fluid particle. The equation is defined by pressure p, viscous stresses τ, density ρ, velocity vector u and the a source term for body forces Sm (Versteeg & Malalasekera, n.d.). The last equation, Eq 5.3, conservation of energy, based on the 1st law of thermodynamics and states that the rate of change of energy in a fluid particle is equal to the rate of heat addition to the fluid particle plus the rate of work done on the particle (Versteeg & Malalasekera, n.d.). The equation is defined by the sum of internal and kinetic energy E, rate of heat addition $k\nabla T$ and a source term Se.

$$\frac{\partial \rho}{\partial t} + \nabla \cdot (\rho \boldsymbol{u}) = 0 \qquad \text{Equation 5.1}$$

$$\frac{\partial \rho \boldsymbol{u}}{\partial t} + \boldsymbol{u}\nabla \cdot (\rho \boldsymbol{u}) = -\nabla p + \nabla \boldsymbol{\tau} + Sm \qquad \text{Equation 5.2}$$

$$\frac{\partial \rho \boldsymbol{E}}{\partial t} + \nabla \cdot (\rho E \boldsymbol{u}) = -\nabla \cdot (p\boldsymbol{u}) + \nabla \cdot (\boldsymbol{\tau} + \boldsymbol{u}) + \nabla \cdot (k\nabla T) + Se \qquad \text{Equation 5.3}$$

CFD algorithms can solve a wide variety of problems and must be tailored to the task at hand. To do this one has to, somewhat, anticipate the flow phenomenon occurring to correctly select the settings in the selected solver. A flow domain is generally referred to the physical space and its boundaries that is to be modelled, and for this thesis external flow domains are used. External flow domains are defined as unbounded space that surrounds an object, for example a bird or a feather in flowing air. Domains have to be discretised both space and time to allow for the mathematical algorithms to calculate accurate results. This means that the domain has to be divided into smaller parts where the algorithms have to be solved for each part and time has to be iterated in small increments to accurately capture the flow behaviour. The more complicated the flow is or the more intricate the object is the smaller the space and time is discretized, which in turn increases the computational costs, both in number of CPUs and CPU hours. The settings used in models have to be verified, where the discretization is analysed and verified.

5.1.2. Computational solid mechanics

Solid mechanics studies the behaviour of solid materials, i.e. the motion and deformation of a body subjected to force. The behaviour is dependent on the geometry, material properties, boundary and loading conditions (G. R. Liu & Quek, 2013). These systems quickly become complex and numerical methods are often necessary to solve a set of force equilibrium equations. One such method is the finite element method (G. R. Liu & Quek, 2013) (FEM), which discretise the domain into finite elements on which the equations are numerically solved. The force equilibrium equations are based on Newton second law and are described by a set of differential equations (G. R. Liu & Quek, 2013) (Eq. 5.4 and 5.5) which describes how the stress tensor $\boldsymbol{\sigma}$ and external forces $\mathbf{f}_b$ are related to the second time derivative of the displacement $\mathbf{u}$ and the density ρ.

$$\boldsymbol{L}^T\boldsymbol{\sigma} + \boldsymbol{f}_b = \rho\ddot{\boldsymbol{U}} \qquad \text{Equation 5.4}$$

$$\nabla\boldsymbol{\sigma} + \boldsymbol{f}_b = \rho\ddot{\boldsymbol{U}} = \rho\frac{\partial^2\boldsymbol{u}}{\partial t^2} \qquad \text{Equation 5.5}$$

5.1.3. Fluid structure interaction models

For highly complex systems, where both deformation in the solid and corresponding change in the fluid response is important to capture, standalone computations cannot capture all aspects. This is especially true in a feather that can bend and twist, therefore another type of computational model is needed. A fluid-structure interaction (FSI) analysis is an analysis to determine how a fluid impact the structural deformation and is the combination of a structural- and fluid- analysis.

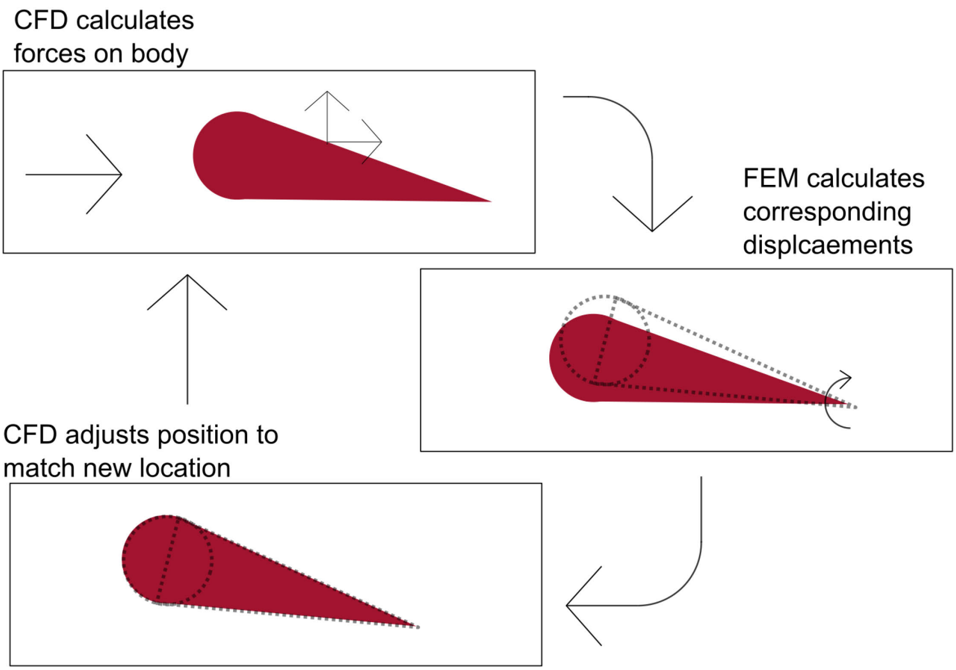

Figure 5.1. Schematic illustration of the iterative process when data is transferred between the different solvers.
The fluid dynamic domain calculates the forces on the body from the flowing fluid, these are then transferred to the solid dynamic solver and the corresponding displacements to the forces are calculated. The displacements are then transferred back to the fluid solver where the fluid domain has to adjust to the displacements, and then the forces on the new setup can be calculated.

To perform this type of analysis an interface where the surface of the solid meets the fluid needs to be established. As a fluid moves over a solid object it exerts pressure on the solid surface, if this pressure overcomes the equilibrium state of the solid object it must move to remain its equilibrium. Practically, figure 5.1, this means that pressure calculated in the fluid computational domain must be transferred to the solid computational domain. In the solid domain the corresponding displacement is calculated and transferred back to the fluid computational domain. In the fluid computational domain, the interface must then adapt to the new boundary. In essence this means that the process is iterative in more ways than one. The separate domains are stepping time forward with a time step set to resolve the flow phenomena and capture the solids behaviour, and data is transferred back and forth between the solvers. The time increments to drive the time forward and the exchange of data typically comes with high computational costs.

5.2. Computational models

The computational modelling only works if a computer model exists that the applications can base its algorithms on. The base of the models used in this thesis is based on a CT scan (figure 4.1 and figure 5.2) of the ninth primary flight feather from a Jackdaw (*Corvus monedula*). The CT scan was done using the ZEISS Xradia XRM520 Submicron Imaging System (http://www.zeiss.de/) at the 4D Imaging Laboratory, Division of Solid Mechanics, Lund University, with a resolution of 10 µm/voxel. The CT scanned feather is 170 long and 14 mm wide at the widest point. Note that there are natural deviations from these measurements and can differ between both wings on the same feather and between individuals in the same species (Polo & Carrascal, n.d.).

The CT scan is the base of two main models, created in SolidWorks 2025 (Dassault systems Waltham, Ma, United States. The first is a smaller model of a part of the feather for standalone fluid dynamic analysis where it is possible to investigate smaller details of the feather and a second model of the outer part of the feather for more complex FSI analysis, where the overall behaviour can be studied.

5.2.1. Paper 1 and 2

The partial feather model build

The three-dimensional model for **paper 1** and **paper 2** was based on a cross-section of the feather (figure 5.2) located in the open slotted part of the wing and subjected to oncoming flow without support from adjacent feathers. The cross section (figure 5.2 c) contains the outline of a posterior and anterior barbs, shaft and barbules.

Although a cross section of the feather contains the cut of several adjacent barbs, it was assumed that they are similar enough to use to create one singular barb. Therefore, the outline of these barbs was extracted from the cross section and repositioned at the correct depth, so they form a continuous single barb. This barb was then copied and repeated along the shaft creating a continuous vane. The shaft, although changing throughout the length (figure shaft cross section) was assumed constant in small sections. This approach also make it possible to create a cyclic domain, producing a pseudo-infinite span that eliminates end effects that would otherwise occur, which is not representable for the behaviour of a bird feather. Additional simplifications were made to the treatment of the barbules. They are too small to spatially resolve properly and where therefore approximated with a plane with its top surface matching the upper placement of the barbules. In this manner, the single cross section of the feather was made three dimensional and represents the characteristics of the CT scanned feather. The process to create this base model was described in **paper 1**.

This model represents a smaller section of the feather, instead of a larger section or the entire feather. The measurement for the base feather model was 13.2 mm wide (chord), shaft was 1 mm wide and high, and the angle of the anterior barbs are 17 degrees and 29 degrees for the posterior barbs. The position of the posterior vane was the average of 5 individual feathers, where one is the CT scanned and 4 are surface scanned feathers with a lower resolution scanner. The average of several feathers was done to reduce the chance of impact from natural variation of vane shape and warping.

In addition to the base feather model (FM), for **paper 1**, a feather equivalent aerofoil (FEqA) was created, with the intention to create a streamlined foil that maintained the flow response as the FM to further investigate the impact of the feather components on the flow. The FEqA outline was based on the results from the FM, where several recirculation zones were detected, the surfaces was chosen so that the top surface was in line with the top of the barbs as well as the shaft and the bottom surface was along the line where the divergence of the Lamb vector (Hamman et al., 2008) ($Lamb = \omega \times U$) was 0, at the zero lift angle (α=-2.59º). This criterion indicates that the flow is irrotational (Hamman et al., 2008), which could be interpreted as the true flow interaction surface where all the structures created by the shaft and barbs are encapsulated.

For **paper 2** a more in-depth morphological study was created, the morphological changes were grouped into three subsets, barbule height location, barb angle and shaft height were changed to study the flow response. This was done by using the base model moving the barbule position along the barb height, changing the barb to shaft angle whilst keeping the width of the vane and reducing the shaft height, see **paper 2** for details.

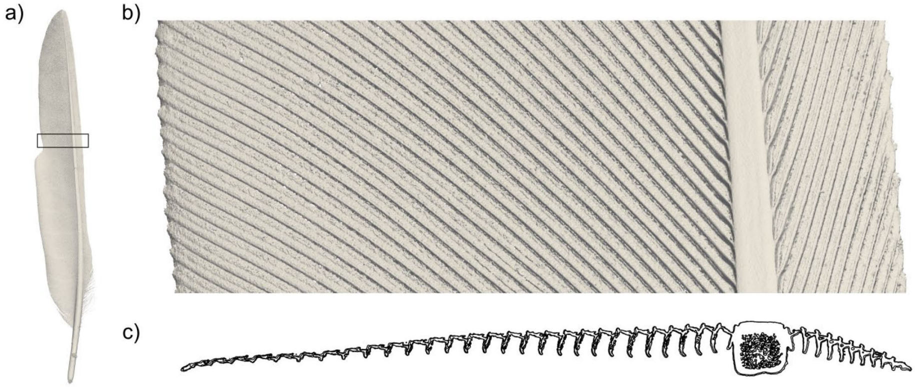

Figure 5.2. CT scan of Jackdaw feather
a) Dorsal view of the CT feather, black box shows location of magnification
b) Magnification of the CT scanned feather, lines show dorsal ridge of barbules
c) Cross section, on the shaft and barbules. Partially reworked from paper1.

Simulation model

A bird has many flight patterns, the two main ones are flapping and gliding, flapping is the motion when the wings are moving to create lift and thrust and gliding is when the wings are held in a fixed position. This study was made using the gliding flight pattern. The flow properties for a feather of this size are interesting. A Jackdaws glide speed is approximately 8 m/s (KleinHeerenbrink et al., 2016), which translates to a Re~7000. At these conditions the flow and boundary layers are laminar, which makes it unsuitable to use turbulent modelling. However, the flow may separate, especially at higher angles of attack and then it is possible to have a turbulent wake, therefore the setting on time and space are important and selected to capture turbulence when present.

Simulation in **paper 1** and **paper 2** has been performed with OpenFOAM8 (openfoam.org) and all meshes where created in Hypermesh 2025 (Altair, Troy MI, United States). The reference simulation model was validated by a mesh sensitivity study where three mesh size settings were investigated for three angles of attack. The result deviation was less than 3% for the two finer meshes so the middle mesh was selected. The solver settings were investigated by setting up an Eppler 387 aerofoil and comparing it to wind tunnel results (McArthur, 2008). Simulated results show quantitative adherence to wind tunnel data. However, further simulation with additional aerofoils (Levy & Seifert, 2009; Sauvageat, 2016; Winslow et al., 2018) compared to simulation data, suggest further experimental studies on E387 at low Re are necessary. Se **paper 1** for details.

Results have been studied for a range of angles of attack. The base FM has been investigated for a larger angle of attack range -4.59 – 20.41, whilst the feather equivalent model as well as the modified feather models in **paper 2** has been investigated for angles of attack ranging -2.59 – 10.41.

When evaluating the flow, traditional engineering metrics for aerofoils have been utilized, which are based on the lift, drag, and pressure coefficients as well as looking at the separation points and torque around the shaft.

5.2.2. paper 3

A FSI model, consisting of two different solvers, is a more complex setup than a stand-alone setup, where only one solver is used. The FSI approach is however necessary when an object dynamically changes shape over time when exposed to loads, as a feather does. FSI simulations, which are setup consecutively, meaning one solver is working at the time as is used here, the computational demands can be high. Additionally, the different solvers have different requirements for optimal performance, which means that compromises often are necessary.

Build of feather model part

The model for **paper 3** and **paper 4** was based on the same CT scanned feather as in **paper 1** and **paper 2.** However, for this model only the part of the feather that is located in the slotted part of the wing was included in the model. To create a model seven construction cross sections located from the notch out to the tip of the feather, was extracted from the CT scan. Each of the seven cross sections profiles was connected using SolidWorks loft tool. However, instead of modelling each barb individually, all barbs were encapsulated into a sheetlike structure where the dorsal and ventral surface matches the top and bottom of the barbs, figure 5.3. This was done for both the leading and the trailing vane, whereas the shaft was modelled as solid after the outline of the shaft. The aerodynamic performance of the encapsulated model was evaluated by the same process as presented in **paper 1** and **paper 2,** and found to be qualitative accurate, so this setup was used moving forward.

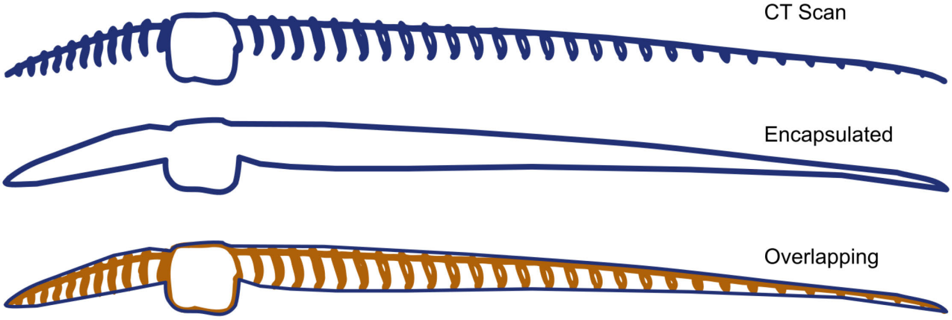

Figure 5.3. Cross section of the CT scanned model and encapsulated model.
On top the CT scanned model cross section outlining each barb and barbules. Below, the encapsulated model's cross section where the barbs and barbules have been encapsulated into a single structure.

The feather model was divided into three main parts, the leading vane, shaft and trailing vane, since the material properties on these three parts vary. Additionally, the shaft have changing properties along the length of the shaft, and is stemming from the changing cross section, figure 4.1 and figure 4.2, including the shape and the interior hollowness. To be able to take this into account the shaft was further subdivided into eight parts. This is a simplification of the feather that has implications for how the material properties needs to be setup. The encapsulation of the barbs into a sheet adds mass to the vanes and modelling the shaft as a solid adds mass to the shaft. In the case of the shaft, increased material also increases the second moment of area. Both aspects have to be accounted for in the material setup. However, due to computational cost and complexity of the solid and the fluid dynamic models, as well as little knowledge how the barbs move under load, and how much force is necessary to separate to adjacent barbs, this approach was chosen.

Material setup

The feather has a high complexity resulting from the hierarchical and interconnected structure between the shaft, barbs and barbules, as well as the internal lattice of the keratin fibres inside each part. In combination with the simplifications made, the resulting material in the model was set to be anisotropic to be able to imitate the movement of the feather. For anisotropic materials, the stiffness E, Poisson's ratio, v, and the shear modulus, G, as well as the material directions, must be defined. Starting with the shaft, E is assumed to be constant, whether it is so or not is unknown and conflicting data exists (Bachmann et al., 2012; B. Wang & Meyers, 2017). I is directly dependent on the cross section of the object, and if it is hollow or not, and I therefore is different over the shaft length. Structural dynamic solvers calculate I and area directly from the geometry, and in this case the simplified geometry was not representative of the real feather geometry. For the shaft, I can be regulated by scaling E, using the ratio between I^{solid} and I^{hollow}, since it is the bending stiffness EI that is used by the force equation in the solver. The calculation of I was based on the method presented in (Purslow & Vincent, n.d.). The simplifications made with the encapsulation of the vanes and the limited material data; the material properties values were based on the shaft properties.

The mass can be regulated by scaling density based on the area covered by solid material vs no material or medulla. The solid part of the shaft ranges from 53 – 100% of each modelled shaft subpart and the reference density is 700 kg/m^3 (Weiss & Kirchner, 2010). The relative density of the vanes is based on the area occupied by the barbs in the base cross section vs the overall encapsulated area (19.6 and 18.9% for the leading and trailing vane, respectively). This gives a density of 137.2 for the leading vane and 130.2 for the trailing vane.

The shaft is not straight and has a built-in twist (figure 4.2), and the barbule in the vanes has at set angle in relation to the shaft. With anisotropic materials the direction of the material is important, therefore a local coordinate system needs to be defined for each part to correctly represent the material. For the shaft, the first direction was set along the shaft, the second direction was from side to side (anterior to posterior), and the third direction was set up and down (dorsal to ventral). For the vanes the first direction is set with the same angle as the barbs are attached to the shaft, 17 and 29 degrees for the leading and trailing vane, respectively. The second direction was in the dorsal-ventral direction and the third direction is in the remaining direction. Due to the high flexibility and low buckling tendencies of the feather it is assumed that the Poisson's ratio is zero for all v in the vane and for the shaft v12 and v13 is set to zero and v23 is 0.4 (Bachmann et al., 2012) . The shear modulus G's initial value, 1.4e9 GPa, is based on the isotropic equation, eq 5.6, with ν=0.4 and E=4e9 GPa, table 5.1. The isotropic relationship does not have to be true for an anisotropic material, and with the high flexibility of the feather in multiple direction it is possible it needs to be lower to allow the material to deform the amount necessary. In the vanes, the values were assumed to be lower than the isotropic relationship and the desired sweep motion is controlled by G13 and G12 or G23, which are set to a similar value as a start point. For the shaft, shearing was not expected in the G23 direction, so that was set to the isotropic relationship, whilst the potential shear is higher in the other two directions. However, using the cross sections of the shaft to evaluate the behaviour it was assumed that G12 < G13. The starting values of the material properties as set for the reference case is summarized in table 5.1. Note, that for the shaft, these are the values that represent a cross section where it is entirely solid. Where the shaft is not, the values are modified according to the E and density ratios, see **paper 3**, for details.

$$G = \frac{E}{2(1+\nu)} \qquad \text{Equation 5.6}$$

Where G is the shear module, E is the Young's modulus and v is Poisson's ratio.

In addition to the material properties already defined, another aspect has to be considered. Feathers in general, have shown features that potentially dissipate energy, for example owls flying silently (Gao et al., 2015) or structural damping from barbs and barbules moving (Deng et al., 2023). Although, no data has been collected from a jackdaw, damping properties have been investigated on a pigeon (Deng et al., 2021) and based on that study the Reyleigh damping was calculated. Using the tip frequency of 6.46 and 8.16 and an average damping ratio of 3.8 percent (Deng et al., 2021), the damping coefficient are estimated to $\alpha = 1.72$ and $\beta = 8.3e-4$.

Table 5.1 Material properties for reference case
Table showing reference material setup for vanes and shaft, shaft material is modified for each part.

	E1	E2	E3	ν12	ν13	ν 23	G12	G13	G23
Vanes	4e9	4e9	4e9	0	0	0	14e5	1.4E5	1.4E5
Shaft	4e9	4e9	4e9	0	0	0.4	1.4e6	1.4e7	1.4e9

Simulation models

The final setup of the model is a fluid-structure interaction (FSI) model. It is a partitioned approach set up consecutively running one computational model at a time. The fluid dynamic simulation is performed with Simcenter STAR-CCM+ 2022.1 Build 17.02.007, Siemens digital Industries Sofware, Plano, TX, USA and the structural dynamic simulation was performed with Abaqus/Standard v.2023, Dassault Systèmes Simulia Corp., Johnston, RI, USA. The simulation setup for each solver was checked prior to the FSI setup, the fluid simulation was checked by a mesh refinement study were the pressure and velocity was monitored around the model as well as the aerodynamic forces. For the structural simulation, mesh was checked by monitoring the exited frequency modes, see **paper 3** for details. When the two solvers were combined to the FSI setup, it was validated against experimental data. Note that the feather used for experimental test was not the identical feather used for the CT scan-based model, but still a 9^{th} primary Jackdaw feather. The experimental setup was a feather mounted in a wind tunnel (Pennycuick et al., 1997), and the displacement and angle of attack was monitored with a high speed camera system (two LaVision Imager pro HS 4M, 2016 x 2016 pixels, LaVision, Gmbh, Goettingen, Germany). 15 points were monitored by manually tracking setup in Matlab clicking_gui_two_cams, a custom written Matlab software by Dr Simon Walker (Walker et al., 2009))

To mimic gliding flight conditions the velocity of the simulation domain was set to 8 m/s (KleinHeerenbrink et al., 2016), which is equivalent to Re =7600, with the modelled feather base chord at 0.015 m. Due to simulation startup stability, the flow is ramped with a linear ramp from 0-8 m/s over the first 0.05 seconds, which corresponds to 26 c/U. The time step was set to 4.5e-6 seconds and the simulation time was 0.153 seconds (80.5 c/U). Note, that the CT scanned model is scaled by a factor 1.17 in all directions, to better fit the measurements of the feather used in the experiments. The wall the feather model (figure 5.4) was mounted to was set with slip conditions, the wall back of the feather was set to a pressure outlet, and all other walls was set to a velocity inlet.

Data was collected at 9 cross sections in the feather model (collocated with the shaft subparts. At each cross section 8 points of data were recorded, on point at the leading and trailing edge, two at the base of each vane where the shaft and vanes attach, and one point at the top and bottom of the shaft. At these points the coordinates of each point were tracked allowing for displacements, pitch angle and camber to be estimated. This data was then compared to experimental data from a wind tunnel, additionally, in the simulation forces on the feather were tracked.

Figure 5.4. The feather FSI model mounted to the wall, in resting position.

5.2.3. Paper 4

The model for **paper 4** was based on the same principals used for **paper 3**, therefore only the differences will be presented in this section. The main differences between **paper 3** and **paper 4** are that in **paper 3,** the material properties was the focus, and in **paper 4** a morphological study was done.

The feather has a built-in pitch up twist, figure 4.2, and consequently the CT based model for **paper 3** and **paper 4** also has this twist. Each construction cross section has a built-in geometry angle compared to the base chord line. This geometry angle was modified in steps of 33 %, based on the CT scanned feather versus a completely untwisted feather. Each construction cross was twisted in steps, so that the relative twist of the modelled feather was change. The result was 5 models where the twist was 0% - 133%, where the modification with 0% twist did not have any twist, 100%

was the unmodified CT based model and the modification with a 133% twist was twisted more than the CT based model.

The material is setup the same way as described for **paper 3**. However, only one of the tested material property combinations was selected as settings for this paper. The selected properties were the ones corresponding most accurately to the experimental data, see table 5.2 for material properties.

In **paper 3** a linear ramp was used to ramp up the flow for startup stability, however it was observed that there was a slight overshoot of the displacement of the feather. To decrease this overshoot, and consequently reach a stabilized solution faster, the linear ramp was switch to a linear ramp with an elliptic end phase. The ramp up time was the same as in **paper 3**. Additionally, twist modifications 33-133% was simulated using 4 m/s as air speed.

Table 5.2. Material settings on vanes and shaft for paper 4
All stiffness, Poisson's ratio and shear modulus material properties for both the vane and base values for the shaft, for all 3 directions.

	E1	E2	E3	ν12	ν13	ν 23	G12	G13	G23
Vanes	4e9	4e9	4e9	0	0	0	14e3	1.4E4	1.4E5
Shaft	4e9	4e9	4e9	0	0	0.4	1.4e6	1.4e7	1.4e9

6. Results

A summarised version of the results from each paper included in the thesis is presented in this chapter.

6.1. The flow around a feather section (paper 1)

In **Paper 1**, a thorough investigation of how the air moves around a feather section was performed and it is uncovered that the flow patterns are complex, especially on the bottom side of the feather. This complexity indicates that the effective surface of the feather was not outlined by the feather itself but by the feather and the flow structures surrounding the feather. There are several rotating structures under the barbules in front of the shaft and a larger rotating structure behind the shaft (figure 6.1 a) pushing the effective surface out from the feather model. This interpretation was investigated by using the model that creates a more aerofoil like surface, the feather equivalent aerofoil (FEqA), described in the method section.

The response of the modelled feather shows a lift and drag curve (figure 6.1 c) that have similar behaviour to engineered aerofoils and matches the performance for similar Re and construction (camber, thickness). Time series of the lift curves show three distinct oscillation patterns associated with a range of angles of attack, $\alpha \leq 4.41$, $5.41 < \alpha \leq 10.41$ and $a \geq 15.41$, respectively. These groups are associated with the flow three distinct separation points, trailing edge, back end of the shaft and the leading edge. These separation points are also strongly linked to the shedding patterns and the subsequent fluctuations in the lift and drag coefficient response.

On the ventral side, the flow patterns are complex, on the leading vane (figure 6.1), rotating structures are located close to the lower edge of the barb, in the space between the barbs. When the flow reaches the shaft, the air must move under it, and the large backward facing step at the end of the shaft forces the flow to separate from the feather surface. This in turn creates a large rotating structure under the first half of the trailing vane. The air flow direction between the barbs on the trailing vane was not uniform. Depending on the pressure distribution, the flow either flows towards the shaft or away from the shaft, depending on the position along the barb.

The pressure distribution (figure 6.1**)** changes characteristics as the angle of attack increases, both on the leading and trailing vane, reflecting the changing position of the separation point and the shedding pinch-off point. The subsequent centre of pressure was not collocated for all angles of attack, however, for 3.41 ≤ α ≤15.51 they are closely located at approximately ~0.4 x/c. The resulting pitch moment has two distinct curves, one for α≤5.41 And one for α>5.41.

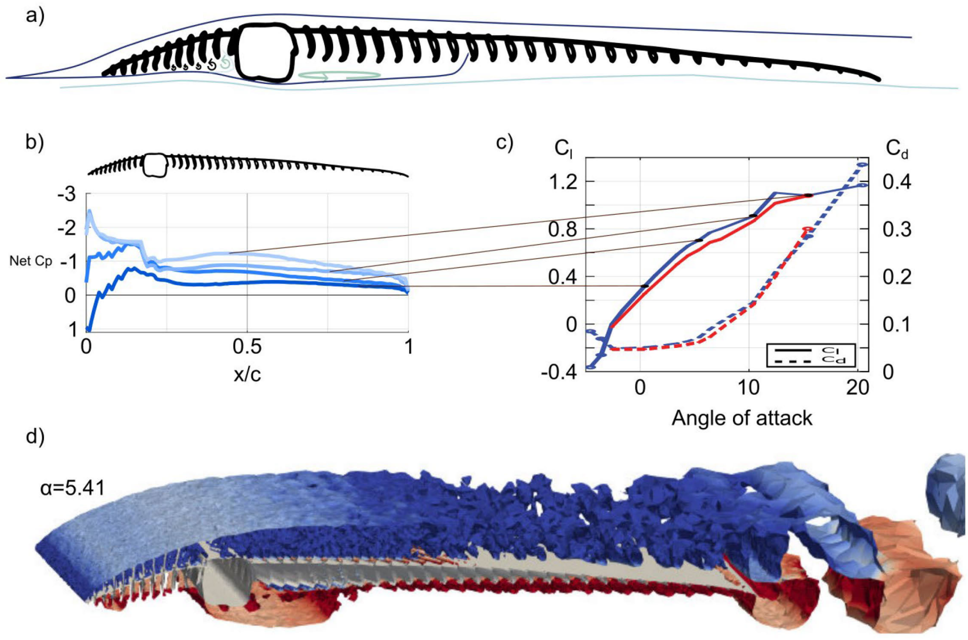

Figure 6.1. Summary of the results from paper 1

a) Schematic flow patterns around the feather. Separation points differ.
b) Net Cp for feather, at different angles of attack, see c)
c) Cl and Cd for both the FM model (blue) and FEqA (red)
d) Visualization of the shedding patterns

The feather equivalent aerofoil (FEqA) aims to include all the recirculating structures under the feather, as well as the barbs and shaft on the top side to create an aerofoil object. This larger profile shape allows the flow to pass around the profile with minimal disturbances while maintaining the same properties as the feather. The overall result from this model was that that the flow characteristics and resulting behaviour was similar to that of the feather model. Nevertheless, differences are detected between the two models and noticeable with lower lift and drag for the FEqA model. With a smooth dorsal surface, the flow separation points are less distinct, and the fluctuations seen in the lift curve transitions at different angles. The difference in separation points also impact at what angle of attack the shedding starts. The smooth surface profile of the FEqA, also reflects in the pressure distribution, where the distinct effect of the shaft was lessened and a smoother transition from the leading vane over the shaft to the trailing vane was observed.

The centres of pressure are grouped at 0.34 x/c somewhat forward of centre of pressure grouping of the feather section model. Overall, since the structures obstructing the flow are removed the flow has less disturbances than the feather model.

6.2. Response to morphology changes (paper 2)

In **paper 2**, the flow response to modifications of the base CT feather section model has been explored. The modifications have been categorized into three groups, the first two modifications investigate the depth to width ratio between the barbs and barbule plane, and the third group investigates the shaft profile. In the first group, the barbule plane is moved along the height of the barbs, which creates different depths of the wells between the barbs. In the second group, the barb angle was changed, which makes the barbs closer or farther apart, and in the third group the shaft is cropped to create a more aerodynamic profile. The modifications have been evaluated by comparing the integrated lift-to-drag ratio ($(C_l/C_d)_{sum}$) as well as the maximum value of lift-to-drag ratio ($(C_l/C_d)_{max}$), summarized in figure 6.2, reworked from **paper 2.** A higher value, in the presented ratios, suggests a higher aerodynamic efficiency. Additionally, the pitch moment has been analysed, and all the cases evaluated have a distinct two slope appearance where the change in pitch slope is found around a=5 degrees, close to the estimated $(C_l/C_d)_{max}$.

Barbule plane

For this group of modifications, the barbule plane was moved along the hight of the barbs. First, considering the modification on the trailing vane, the aerodynamic efficiency performance was worse as the plane was lowered, which increases the distance between the plane and the top of the barbs. On the one case where the barbule plane was elevated the aerodynamic efficiency was increased. Secondly, when lifting the barbule plane on the leading vane, the performance went down, compared to the base CT feather model. This is associated with a dip in lift coefficient at a = 4.41 and a=5.51.

Regarding the spanwise flow on the dorsal and ventral side of the trailing vane, the overall location where the flow changes direction as well as the intensity is similar to the reference CT scanned feather. However, the lower the posterior barbule plane was located, the greater the effect on the flow above the plane, which consequently impacts the lift and drag.

Barb angle

For all the modifications where the barb angle was changed, the values for $(C_l/C_d)_{max}$ and $(C_l/C_d)_{sum}$ are worse than the base CT feather model case (figure 6.2). This stems from a dip in C_l, and higher C_d in mid-range angles of attack. Changing the distance between the barbs, by changing the angles, changes the balance in the flow and the position where the flow changes direction in the space between the barbs. The wider the channels the higher the spanwise velocity, **see paper 2**.

Shaft height

Removing a large part of the shaft that protrudes below the vanes of the feather model, changes the flow paths, particularly under the feather model, as well as the flow direction between the barbs. This in turn effects the pitch moment and the two slope characteristics changes to three slopes instead. This modification shows better $(C_l/C_d)_{max}$ $(C_l/C_d)_{sum}$ than the base CT feather model, however, the $\alpha_{zero\ lift}$ has shifted, which narrows the operational length since the angle of attack which the modified feather produces lift increases.

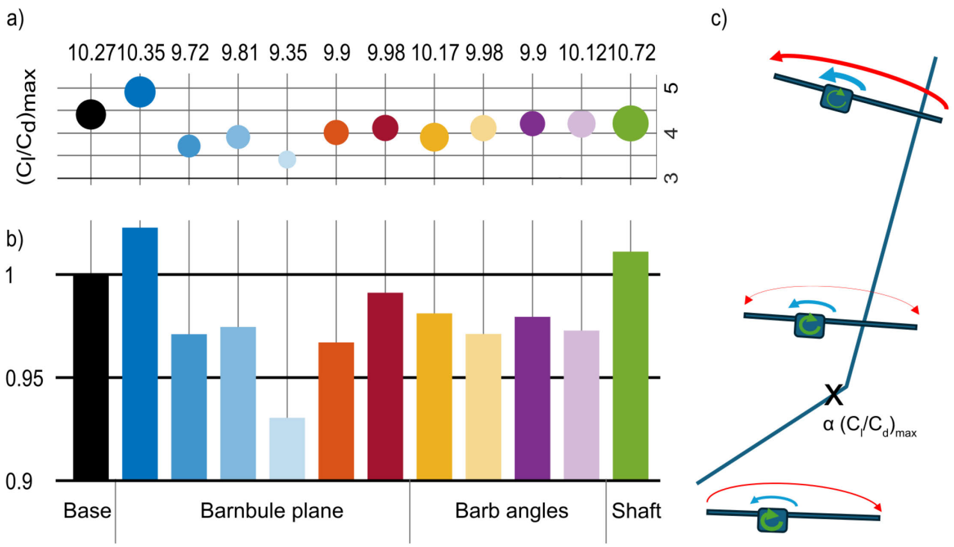

Figure 6.2. Results from paper 2, reworked from paper 2

a) $(C_l/C_d)_{max}$ for all cases, dot size indicate relative magnitude and presented in the value above the hart. the right axis show at what angle of attack the maximum was.

b) $(C_l/C_d)_{sum}$, the integrated value of the lift-to-drag ratio for all cases, normalized with the CT reference case.

c) Schematic image of proposed mechanism for passive pitch control.

6.3. Response to material properties (paper 3)

In **paper 3**, the response of the distal part of the feather, to changing material settings in the vanes and the shaft was explored. The feather has two different states, one unloaded and one loaded, where the difference is whereas the wind is blowing or not. In the loaded position, the base test case had an upwards bend of 13.4 mm (experiment = 10.9) and backwards bend of 4.1 mm (experiment = 9.3 mm). The change in pitch angle of the feather was 1.2 degrees for the first 6 cross sections and 3 degrees higher for the rest of the cross section compared to the unloaded state. The first 6 cross sections were in line with the experiments, and the outer 3 show an increase rather than the decrease in pitch angle found in the experiments. In the base setup the backwards sweep is the variable that was the furthest from the experimental setup. The general flow over the feather model, contains large shedding structures from the middle of the feather and distally as well as a tip vortex (figure 6.3), these shedding structures reflected in the force monitors (figure 6.3).

The modifications of the material properties have been divided into three groups; changes to the shear module on the vanes, changes to the shaft properties and miscellaneous changes. The results are evaluated by tracking the displacement, pitch angle of the feather and shaft, the camber and the forces on the feather. A summarized version of the results in **paper 3** will be presented, see manuscript for details.

Changes on the shear module on the vanes

Changing all shear variables at once by decreasing the values, gives a less ridged response of the feather model. The least stiff of these settings, increased the distance of the min/max values from the mean, had more upwards bend and lower angles of attack then the reference case. When changing one shear module variable at a time, the response affected primarily one property at the time. Decreasing G12, lead to a better response in sweep, figure 6.3, which also improved the agreement with the experimental value. Decreasing G13 mainly had an impact on the camber, increasing the values. Finally, decreasing G23, had a slight negative impact on the sweep, reducing the agreement with experiment, as well as reducing the angle of attack and lift and drag forces.

Changes on the shaft properties

Changes to the shaft properties, were made on both the shear module and the stiffness of the shaft. Lowering the shear module and stiffness of the shaft made the response, ultimately, less ridged by either increasing the bend or by decreasing the angle of attack, without increasing the backwards sweep. Two main responses were seen, the first was a decrease of the pitch angle and the second an increase of the upwards bend.

Miscellaneous changes

Three different changes were considered, halving the thickness of the trailing vane, removing the damping and increasing the density of the material, thus increasing the weight of the feather model. Halving the trailing vane on the model lowered the angle of attack response. Removing the damping and increasing the density had the same effect, increasing the instability of the time signals. In the case of the no damping, an oscillating pattern was introduced on the displacement time signal. For the case with the density, the amplitude of the oscillations in the force signals was increased, and the signals also showed signs of diverging.

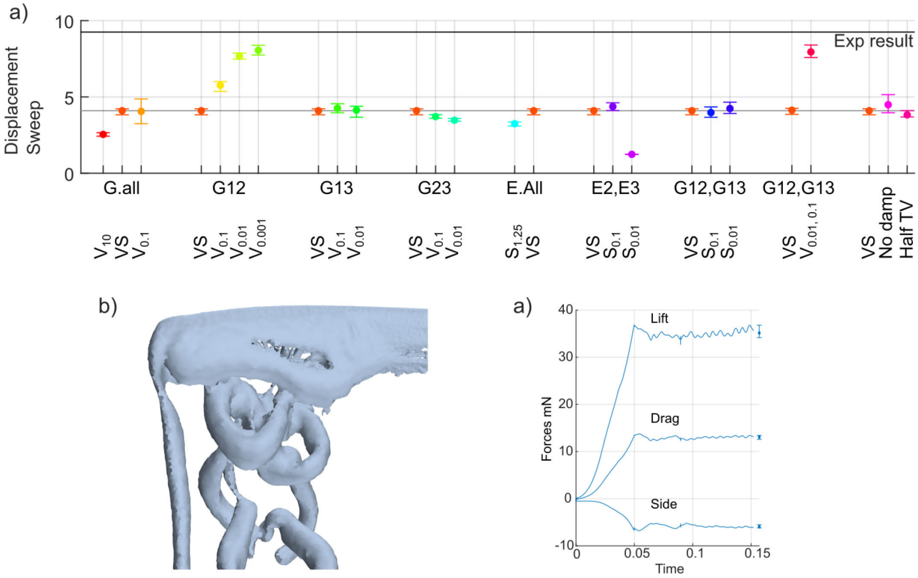

Figure 6.2. Results from paper 3, reworked from paper 3

a) Sweep displacement for all material modifications run.
b) Shedding patterns represented with Q-criterion at value 100000.0 /s^2
c) Force, lift, drag and side, response over time for the base reference case.

6.4. Response to feather untwisting (paper 4)

In **paper 4**, the same feather model setup as presented in **paper 3**, was used. However, the basic reference case was not the same. The selected case was the one behaving most similar to the experimental data. Five different modifications were explored where the inherent twist of the feather had a twist of 0-133%, where the model with no twist was represented with 0% and the unmodified model had a twist of 100%. The general response of the modifications was that the lift and drag showed a reduction with a decreasing twist (figure 6.4). Even though they both where decreased, the drag decrease was larger than for the lift. This also results in a L/D that increased as the feather decreased in twist. Another feature that was noticeable in the time signals for the lift, was the change in frequence in the variation in the signal. The modifications with higher twist displayed a higher frequency

(~180Hz measured for twist 100%) and a lower frequency for the modifications with a lower twist (~33Hz measured for twist 0%).

The response in the displacement did not follow the same decreasing pattern as for the lift and drag. The upwards bend was consistently between 12-14 mm, whilst the backwards sweep decreased, as seen in lift and drag, with approximately 2 mm for each step of untwisting (figure 6.4).

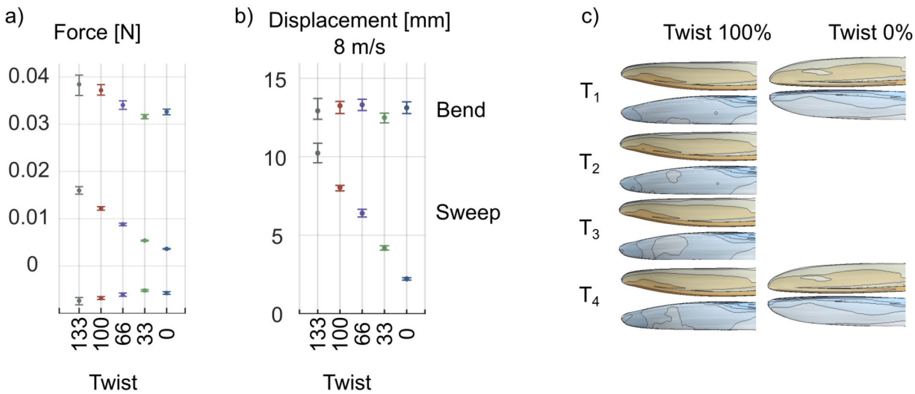

Figure 6.4 Results from paper 4, reworked from paper 4

a) Mean force response for modifications 0-133% at 8m/s.

b) Mean displacement response for all modifications 0-133% at 8 m/s.

c) Pressure distribution for twist 100% and 0% for time t1 = 0.1816 s, t2 =0.1836 s t3 = 0.1849 s and t4 = 0.1867 s.

The reference case, twist 100% shows a small difference in the angle of attack between the resting and loaded case, with a slight lowering of the angles for the proximal cross section. As the feather was untwisted the angle of attack increased in the loaded state, compared to the resting position. On the contrary, when the feather was twisted more the angle of attack did detwist for all the measured cross sections.

The pressure distribution as well as the shedding patterns changed with the twist, which was also reflected in the time signals for the force. In the pressure distribution, figure 6.4, for twist 100%, a shifting pressure was seen, especially at the outer part of the feather (figure 6.4). Comparing the pressure distribution of twist 100% and twist 0% (figure 6.4), over the same time frame, the shift in the pressure is much smaller in line with the oscillating patterns seen in the time signal for the lift.

Lastly the effect of speed was examined, where the air speed was lowered to 4 m/s for modifications 33-133%. The response in the displacement was four times lower than the original model, consistent with the reduction in aerodynamic force (∝**u**2, where **u** is the local speed). The patterns in the displacement were the same as for 8 m/s, where the upwards bend was similar for all modifications and the backwards sweep was lowered stepwise with the untwist. The angle of attack also showed the same patterns as the case with higher speed, if the angle increased with higher speed, it also happened for the case at the lower speed, just to a lower degree.

7. Discussion

At first glance one may think that the feather construction is quite straight forward, and in some respects it is. It is made up by three parts (Lucas & Stettenheim, 1972) with a hierarchal growth pattern where the barbules interlock to create the vanes (Ennos et al., 1995; Feo & Prum, 2014; Lucas & Stettenheim, 1972). However, the deeper you look, the increasingly more complex it becomes. The basis for the complexity are the large displacements possible (Carruthers et al., 2007; Oorschot et al., 2020), whilst withstanding a complex varying force distribution (H. Liu et al., 2024) (**paper 3** and **paper 4**). Furthermore, the feather structures have intricated inner structures that on its own is complex by default (Hendrickx-Rodriguez & Lentink, 2025; Lingham-Soliar, 2014; Lingham-Soliar et al., 2009; Prum, 1999), with their changing cross section shapes (Bachmann et al., 2012), medulla filled centres (Hendrickx-Rodriguez & Lentink, 2025; Lingham-Soliar & Murugan, 2013) and varying fibre lattice directions (Lingham-Soliar & Murugan, 2013). Additionally, the part of the feather and the selected operating conditions used as a study object in this thesis, preforms under passive control with little direct control from the bird (Carruthers et al., 2007; Oorschot et al., 2020). This thesis aims to increase the knowledge on the flight feather functions and behaviour, and there are several points of view to consider. In particular, the basic interaction between the feather and the flow, how the feather structures material impacts the feather response and how the morphology of the feather impacts behaviour.

7.1. Air flow around the partial feather model

7.1.1. Method

Using a computational method to create a model has the benefit of having large freedom in geometry creations, especially when the details of the feathers are as small as they are. Physical models are difficult to create with small details, and in an experimental setup the data recorded is limited, at least compared to the information available in fluid dynamic solvers. These two facts in combination made it desirable to create computer models, with the number of modifications that was intended, and the reason why this method was selected. An effect of not having a physical model was the lack of verification of the models. Even if a physical model had been created, the verification between experimental and simulations are precarious at low Re. Studies show that depending on experimental site (Klose et al., 2021; Tank et al., 2017) and what type of simulation (2D or 3D)(Klose et al., 2021), the quantitative results may be the same but the qualitative is not. The verification process becomes complicated when no direct comparison is at hand, we opted to verify the model by testing the stability of the solver, as well as verifying the solver settings with already know profiles. The solver setting was found to be very stable (**paper 1** supplement) and the quantitative results from the verification model was also satisfactory.

7.1.2. General flow

The general flow around the feather, the overall flow characteristics and the flow phenomena that generally occur at the Reynolds number regime of the feather can be described using other types of object rather than feathers, such as or standard aerofoils or plates (Badrya et al., 2018; J. Chang et al., 2022; Chen et al., 2013; Klose et al., 2021, 2025; Spedding et al., 2008; Winslow et al., 2018). This approach has been used several times, both in an experimental setup (McArthur, 2008; Okamoto et al., 1996) and in computational setups (J. Chang et al., 2022; Levy & Seifert, 2009; Winslow et al., 2018), since they are easy to manufacture or create simulation models out of. However, generally the profile of the aerofoils in these investigations are simpler than the profile of the feather (Badrya et al., 2018; Klose et al., 2021) and, the feather has many microstructures that may impact how the airflow interacts with the feather surface (Alenius et al., 2026; Harvey et al., 2023). For example, the dorsal part of the shaft sits above the barbules (Sullivan et al., 2017) forming the dorsal part of the vanes (also shown in **paper 1** and **paper 2)**, as well as protrudes below the ventral site of the barbules (Sullivan et al., 2017). Structures that are not flush with the surrounding feather may have the potential to trigger the flow to separate, which in turn can affect the aerodynamic performance (Badrya et al., 2018; Klose et al., 2021). It is therefore difficult to know if a simpler standard aerofoil is suitable to use when investigating the performance and behaviour of the feather. A more detailed model, as the one in **paper 1** and **paper 2,** therefore add insight into the flow behaviour around the feather. The results in **paper 1** showed that there were flow structures surrounding the feather that pushed the effective aerodynamic surface outwards, creating a shape more in line with traditional aerofoils. However, this shape is dependent on the underlying structures and for studies that intend to explore the behaviour of the feather and the microstructures effect on the flow a more complex profile is needed that the studies on aerofoils and plates (Badrya et al., 2018; J. Chang et al., 2022; Chen et al., 2013; Klose et al., 2021; Spedding et al., 2008; Winslow et al., 2018).

Would it then be possible to create a compromise, i.e. a profile that retains the behaviour of the feather with a simpler profile? We attempted to do so using the feather equivalent aerofoil presented in **paper 1**. It retained many of the behaviours of the feather and showed qualitative similar results (Alenius et al., 2026). However, I argue that the use of a simplified feather model, to a more aerofoil-like structure, is dependent on the purpose of the study. If it is a more general flow behaviour that is sought after, it can be acceptable with a simplification. However, the FEqA lacks the features that could be one of the driving parts in the feather's behaviour. So, in those cases were the behaviour of the feather or the impact the structures have on the flow, a simplification may not be suitable.

7.1.3. The effect of the feather components

When comparing the FEqA to the detailed feather model, the feather model has a distinct point where the flow separates and drag is worse, suggesting the shaft and barbs increase drag (**paper 1)**. Even though the difference in drag is small, it sits in contrast to other biological system that have shown the opposite behaviour. The valleys between the barbs can be compared to features in sharks (Dean & Bhushan, 2010; Harvey et al., 2023; Oeffner & Lauder, 2012) and dragonflies (Kesel, 2000), which have surfaces associated with drag reducing capabilities. However, compared to sharks and dragonflies, the alignment of the barbs is set at an angle to the flow, which does not follow the alignment pattern seen in sharks (aligned)(Dean & Bhushan, 2010) or dragonflies (transvers)(Kesel, 2000). On the other hand, compared sharks and dragonflies, the feather structures appear more in line with blade riblets (Bechert et al., 1997), where an optimum height-to-dept ratio have been found to be drag reducing (Dean & Bhushan, 2010). However, the father structures do not fall into the optimal range (Bechert et al., 1997), thus having a low potential for drag reducing potential. It is possible that the **paper 1** study is too limited, the conditions where the drag lowering mechanism is critical is during other phases of flight or that the drag penalty from the shaft is sufficiently high to mask any drag lowering contributions. Another explanation for the lack of drag reduction is the way air move in the feather valleys. The angle permits the flow to move spanwise, **paper 1** and show a complex flow where the direction of the air in the valley's changes direction. This flow behaviour obstruct the continuous flow over the surface that contributes to the lower drag, as explained for sharks (Dean & Bhushan, 2010). Combining the higher drag and apparent lack of drag reduction from the barbs, it seems that the primary driving force of the appearance of the barbs and shaft are structural, and not aerodynamic. In the case of the shaft, the easiest explanation is that it has favoured structural stability, the square shape of the cross section is suitable to bare high loads (B. Wang & Meyers, 2017). For the barbs, higher structural rigidity with smaller angles (Feo et al., 2015) or developmental constraints may have a role, e.g. how the feather grow in the follicle may prevent the barbules to for a surface at an optimal position (Prum, 1999).

To further explore the feathers microstructures, and their effect on the feathers behaviour the hight-to-dept ratio between the barbs and barbules was studied in **paper 2**. In **paper 2**, the angle of the barbs was also explored, the way the angels were modified also had an effect to the hight-to-dept ratio. However, only a few cases showed lower drag coefficients (**paper 2** modifying the barbule hight), however these cases were also combined with a lowered lift for the critical angle of attack (5.41 degrees). So, either the drag was worse or the lift was lower, so the overall aerodynamic efficiency was lower. The results suggest that the unaltered setup (CT feather model), is one of the setups tested with the highest aerodynamic efficiency. Only one setup was better, where the barbule plane is flush with the top part of the barbs on the trailing vane (**paper 2**). As mentioned previously, it could be that a developmental constraint is the reason that the barbules sit higher up on the shaft. However, another possibility is the higher risk of damages on the delicate barbules if they were to be more exposed, which would lead to shorter moult intervals, which is costly for the bird (Terrill & Shultz, 2023). Both the location of the barbules and the angle of the barbs show signs of optimization by natural selection for aerodynamic performance, having one of the highest aerodynamic efficiencies.

Arguments have been made that the centre of pressure of a feather should be behind the shaft (R. Å. Norberg, 1985). Combine the location of the centre of pressure with the feather's asymmetrical vanes, this should create a pitch down movement, with respect to the shaft. This would increase the passive movement of the feather, compared if the centre of pressure is closer to the shaft, and therefore also how predictable the feather is moving. The result in **paper 1** show that the centre of pressure is behind the shaft for all angles of attack, as suggested in (R. Å. Norberg, 1985), the results from **paper 1** and **paper 2** show that a pitch down moment is induced by the feather model.

7.1.4. Evolutionary implications

From the results in **paper 1** and **paper 2** two properties recur to explain the feathers behaviour, predictability and stability. We argue for a possible passively stabilizing control mechanism, explained by the pitch momentum slopes. Large angles of attack on the flow would induce a pitch momentum to lower the pitch angle of the feather, and at a low angle of attack the large inherent twist of the feather would keep the pitch angle of becoming too low. Another behaviour that seems to be in favour of predictability, is the large dips in C_l seen in the barb angle and barbule plane modifications (**paper 2**). For many of the modified cases in **paper 2**, there is a noticeable dip in Cl, we argued that this is probably due to the flow transitioning from laminar to turbulent mode, due to the fact that the force coefficient curves also start oscillating indicative of shedding (Badrya et al., 2018; J. Chang et al., 2022; R. Å. Norberg, 1985). It is not unheard of in standard aerofoils to have a shift in the lift curve, usually it is an sudden increase connected to the bursting of a laminar separation bubble (Chen et al., 2013; Klose et al., 2021; Spedding et al., 2008). No separation bubble is detected in the feather modifications, but it does not mean that a separation is not present. We have shown in **paper 1** that the flow separates at different location for the feather model than the feather equivalent aerofoil. The rapid change in lift, could change the functionality of the feather, an increase in lift as seen for the aerofoils (Klose et al., 2021; Spedding et al., 2008) can be positive since a small change in angle of attack would give more force for control. However, for the feather modifications in **paper 2**, with a dip in lift coefficient, it would mean a loss of force, close to the angle of attack of max C_l/C_d **(paper 2)**, which we argue are the optimal angle for the feather to be in. This type of dip in a seemingly critical area, seen in the modification, would not suggest a predictable force distribution and may be an explanation on why the unmodified variant of the feather is the one we see today, because it appears to be more predictable for small changes in angle of attack.

Even though the feather model do not share the drag reduction seen in dragonflies (Kesel, 2000), another feature is. As the angle of attack is increased, the time signal shows a oscillating pattern connected to the separation (Badrya et al., 2018; J. Chang et al., 2022; Klose et al., 2025), if you take the mean value of the signal as well as the max and mean values you get the envelope of the force variation. If you compare the force variation between aerofoils and dragonflies you see that the dragonfly has a more consistent increase in the extreme values than for the aerofoil (Levy & Seifert, 2009), which increases steady up to a point and then increases rapidly. The feather model shares the dragonfly's profile for the force variation envelope (paper 1 supplement). Not only showing that the feather does share properties with other biological system, but another suggestion also that the selection pressures has favoured stability and predictability. Examining the flow regime of insects (Vargas et al., 2008; Wakeling & Ellington, 1997), we find that it is similar to that of the Jackdaw feather, in the ultra-low regime (Vargas et al., 2008). So, it is possible that making a study to compare a feather and insects wings could yield interesting results.

Feathers have features that suggest trade-off between the different functions that a feather performs. The drag penalty of the shaft is probably less important than having a strong enough structure that can withstand the structural demands of flight (**paper 1** and **paper 2)**. The results in **paper 2** suggests that unaltered morphology of the feather is one of the most efficient and predictable of the investigated modifications. Also, there is evidence that the earliest living birds, such as Archeopteryx has lower barb angles on the trailing vane (Feo et al., 2015), we also show that such a configuration has lower aerodynamic efficiency and also stronger spanwise flow between the barbs (**paper 2**). Suggesting that aerodynamic efficiency is important in some respects, and that natural selection could have favoured barb angles seen in birds today.

7.1.5. Limitations

The smaller section model, as seen in **paper 1** and **paper 2,** was only setup for one section of the feather where the shaft extends from the vanes. Compare this to a section further out on the shaft where the shaft extends less from the vanes (figure 4.2) and we see that the selected section is the furthest from engineered aerofoils. Thus, the knowledge about how engineered aerofoils behaves is not as transferable to this section as more distal sections on a feather. However, it would still be valuable to explore interactions between the flow and the microstructures on a section were the shaft is less protruding than in the section seen in **paper 1** and **paper 2**.

Our model show potential in investigating the flow structures around a feather section. The spanwise flow seen between the barbs show that 2D representations of the flow around a feather will not give an accurate representation of the 3D dimensionality of the flow structures. The modifications made in **paper 1** and **paper 2** suggest that there have been an trade-off between aerodynamic and structural function as well as aerodynamic improvements compared to earlier birds (Feo et al., 2015). Nevertheless, our model can be improved on, the main simplification we made as the modelling of the barbules. We decided to create a solid sheet instead of the individual barbules. Two of the main drawbacks to this was that the ventral barbule was removed increasing the depth of the channel under that barbule plane (paper 1 supplemental), we argued that this would have little effect since little air flow is present here, however this is unknown. The other drawback was that the gap between the shaft and the barbule that is created by the angle of the barbule. This is documented to have an effect (Eder et al., 2011), and closing the holes decreases the aerodynamic performance (Eder et al., 2011), mainly by increasing drag.

7.2. Aeroelastic behaviour of the feather

In this section the larger computational model of the outer part of the feather is considered. The barbs and barbules were encapsulated in a sheet and the shaft was solid. The computations were run with a fluid-solid interface to capture the aeroelastic interaction in the feather.

7.2.1. Method

In **paper 3**, it is shown that the material of a feather has a complex interaction with the functionality of the feather. An anisotropic approach of the material matrix was necessary to get the model to behave similar to the experiments. This was exemplified in **paper 3**, we showed that values of the shear module were far lower than for an isotropic relationship, additionally, shear module property had different values depending on the direction in both the shaft and the vanes. With that said, upwards bend and angle of attack had a different response, in respect to the reference case, for more than one material parameter. This highlights the importance of knowing the material behaviour of each subpart of the feather. Unfortunately, modelling the feather material was, and still is, a major challenge. Material studies tend to focus on one aspect of the feather, either the shaft (Bachmann et al., 2012; Bonser & Purslow, 1995; Cameron et al., 2003) or the barb (Butler & Johnson, 2004; Ennos et al., 1995; Sullivan et al., 2016). Modelling the shaft, is easier due to the expectation that it behaves like a cantilever beam (Purslow & Vincent, n.d.), and there is engineering knowledge in creating systems with similar build such as wind turbines ('Introduction to Wind Turbine Blade Design', 2023). Being a single part, compared to the vanes that is built by several copies of the same structures (Hendrickx-Rodriguez & Lentink, 2025; Lucas & Stettenheim, 1972), it is easier to map out the cross sections than for the vanes. Nevertheless, due to computational costs, overall complexity and the model simplifications, previous protocols for of how to apply the known material data was limited.

The approach chosen was to make have an initial setup of the material properties and adjust them to make the model behave like the feather in the experiment. The relationship between the shear module variables in the shaft was partly based on the knowledge about the fibre directions inside the shaft (Lingham-Soliar, 2014; B. Wang & Meyers, 2017), and how that effects the behaviour (B. Wang & Meyers, 2017). We selected to model the feather with encapsulated barbs and a solid shaft. This decision added mass and increased the second moment of area to the shaft and vanes. To account for this, the density was adjusted with the help of the area of selected cross sections along the shaft and then scaled. The reference density used was taken from the tail feathers from a peacock (Weiss & Kirchner, 2010), possible not the most representative for a Jackdaw. However, feathers are made by the same keratin (Greenwold et al., 2014; Hendrickx-Rodriguez & Lentink, 2025; Sawyer et al., 2000), and measuring the density of the feather components has its own sets of issues. Even if the shaft is used, it is small, partly hollow (W.-L. Chang et al., 2019; Hendrickx-Rodriguez & Lentink, 2025), partly medulla (W.-L. Chang et al., 2019; Hendrickx-Rodriguez & Lentink, 2025) and solid (figure 4.1a). The size makes it easy to damage, and the cellular medulla could trap air, so we opted to start with a best guess and modified as needed. The second moment of area can be calculated from the CT scan, so the ratio was calculated and applied to the Young's module, which is one part of the flexure stiffness EI. These are initial assumptions and adjustments and refinements are certainly possible.

7.2.2. General behaviour

Investigations of feathers behaviour when air is blowing on them have been done in several different studies, in wind tunnels (Li et al., 2022; Murayama et al., 2021;

Oorschot et al., 2020; Wiswell & Wissa, 2026a) and computationally (Bouard et al., 2024; Fukami et al., 2025; Gamble et al., 2020), with a mix of feather like and aerofoil like objects. However studies that had the perspective of exploring the behaviour the feather were often made aerofoils based on NACA profiles (Bouard et al., 2024; Fukami et al., 2025; Murayama et al., 2021; Wiswell & Wissa, 2026b). Even though our model has not been investigated in a slotted configuration, the reference Jackdaw feather is located there, and lessons learned from this thesis could be used to improve studies on wings with slotted feathers, which used simplified NACA profiles as feathers (D. Liu et al., 2021; Wiswell & Wissa, 2026b). As suggested in **paper 1** and **paper 2**, simplified aerofoils do not fully capture the feather structure effects on the flow and for **paper 3** and **paper 4**, a FSI model is used to capture the expected passive movement of the feather (Oorschot et al., 2020).

Computational models are powerful and can show both the behaviour of the feather and the flow around it, but to be able to utilize them the setup has to be accurate. In **paper 3**, the setup of the model, the accuracy of the material matrix and the behaviour of the feather is explored. The feather model showed a generally stable behaviour, with low fluctuations in displacement and angle of attack. When the mechanical damping was removed or the density was increased (i.e. increased mass) the fluctuations increased and the behaviour became less stable, further suggesting the feathers inherent stable and predictable nature. However, different bird species show different types of energy dissipation described as damping or flutter, owls reduce sound (Gao et al., 2014, 2015), and, for example, hummingbirds can produce sound (Clark et al., 2011; Clark & Prum, 2015). So further exploration of the damping properties is necessary. Focusing on the mass/density aspect of this phenomenon, a lower mass means lower overall weight on the bird, and lower cost (Berg & Rayner, 1995; Sullivan et al., 2017). A lower mass also means that the structural demand on each feather is lower, which could increase the functional limits of the feather.

7.2.3. Importance of material

The material properties affect the behaviour of the feather model, however, for a material as complex as this, it is important to know what parameter effect what response. When you know that you can better balance the parameters for better response compliance. This is especially important for the vane, which is less studied, and simplified in the model, it also and form the better part of the aerodynamic surface. As mentioned, the upwards bend and angle of attack is affected by more material variables than one. With the limited details how to transfer the know material properties to the model, it is difficult to know the balance between these variables without more studies into the material properties of each microstructure of the feather.

Nevertheless, the results (**paper 3)** suggest that the balance is possible to find. In the case of the backwards sweep, only a single parameter had large impact on the results, the shear module G12 on the vanes, which would be the equivalent motion of the barbs moving in parallel, sliding up and down. We assumed that the vane variable G13 also should have had an impact on this motion since that would represent the barbs moving closer together, but it did not have a large effect (**paper 3)**. We know that feathers possesses the possibility to deflect (Oorschot et al., 2020) (**paper 3)**, which implies that the barbs move relative to each other. The angles that the barbs and barbules are laid out in make it possible for the movement (Ennos et al., 1995; Feo et al., 2016), and the barbs can glide along each other without separating the barbules (Ennos et al., 1995). The barbules do attach to each other and it requires force to separate them (Kovalev et al., 2014). The angel of the barbs and barbules also facilitates other necessary functions, for example it allows for easier preening (Ennos et al., 1995). If the feathers are easier to maintain, the overall cost is lower to maintain them. It places the arguments from **paper 1** and **paper 2** in another light, showing that it is not only the aerodynamic function that needs to be considered when evaluating the layout of each feather part. There is a trade-off factor between multiple functions, not only aerodynamic and structural but also a maintenance factor. The lack of response when trying to find the parameter balance to get the correct sweep, and the how the barbs and barbule move, suggest that the model can be improved by splitting the vane into smaller parts where relative movement is allowed.

The behaviour of the feather when the material properties are changed (**paper 3)**, thus guides the understanding of the importance of the material properties of the different substructures. However, the material properties are a function of the model's simplified nature and build, which cannot be directly transferred to the material properties of the feather. Nevertheless, what all material property modifications had in common was that if they were lowered passed a minimum threshold, the integrity of the behaviour disappeared. This meant that the angle of attack was lowered significantly, the upwards bend increased or the loaded position of the feather was no longer stable. This would suggest that, as long as, the feather material property was above this threshold it would have some stable and predictable aerodynamic function, at least for gliding flight, as it is the only flight mode studied here. However, if some other flight mode produces larger forces this minimum threshold would go up. Nevertheless, as long as the feathers in evolutionary early birds had strong enough microstructures and they interconnected to create an aerodynamic surface the natural selection and selection pressure could refine the features to eventually form the feathers we see today.

7.2.4. The effect of untwisting the feather

Untwisting the feather gave better aerodynamic performance than a feather with the twist we see in Jackdaws today (**paper 4**), for example, better lift-over-drag ratios (L/D). This means that the twist in the feather, used as reference, comes at an aerodynamic cost compared to the untwisted ones (**paper 4)**, in gliding flight at the set speed (8 m/s). General studies on aerofoils show declining lift-to-drag ratios for higher angles of attack (Winslow et al., 2018) (and **paper 1**), so from that aspect the results are as expected. However we were expecting a passive detwist in the modifications with high angles of attack to reduce this cost, which have been suggested (Oorschot et al., 2020), and a mechanism we also argued in (**paper 1** and **paper 2**). In the first two papers the location of the centre of pressure and the pitch moment curves suggested that a passive rotation of the feather to an angle of attack to around the max C_l/C_d angle of attack, as to promote stable flight. However, we see little evidence to this in the result (**paper 3** and **paper 4)**. For the unmodified case the angle of attack was the same for both the loaded and unloaded state, for increased twist there was a slight detwisting and for the untwisted cases the angle of attack increased when loaded. There are several possible explanations for the feather not detwisting, and at the current moment, it is difficult to understand what scenario is most plausible, more studies are needed.

Examples of the reasons why we do not see the expected twist. The first possibility, the balance of the material properties was not correct, or that the simplifications do not allow the feather to rotate as it should. Noteworthy here, was that the experiment also showed little tendency of detwisting, at least to the degree we expected (**paper 3**), suggesting that the main explanation lies elsewhere. Second possibility, the mounting of the feather in the wall somehow locks to possibility for the detwist, or if the detwisting is a part of a general rotation that is initiated closer to the root. A complicated action since the base sweep of a flight feather (R. Å. Norberg, 1985) (figure 4.1), make the rotation axis not to be in line with the shaft for each cross section of the feather. Third possibility, the high angle of attack allows for a different shedding pattern that promotes predictability, as exemplified with cell-like vortex shedding (Pandi & Mittal, 2025). Forth possibility, the driving pressure of selection for the angel of the 9th primary feather, is the fact that it is located first, in the slotted configuration. The properties are difficult to understand in a standalone setup where aerodynamic efficiency could be sacrificed for a behaviour that mainly benefits the feather that follows in the slotted configuration.

7.2.5. Evolutionary implications

Keeping in mind the limitation of the material behaviour in the model vs a real feather, there are some possible takeaways. In **paper 2**, we argued that a potential reason for the feather not evolving a solid plane was developmental constraints, however the results from **paper 3** suggest that the ability to sweep backwards is linked to the ability of adjacent barbs to move independently. Such movements could also absorb some of the energy needed to be dissipated, as discussed previously, damping properties in the material matrix are necessary to imitate the feather behaviour. It would also account energy dissipation that is not linked directly to a function (Clark et al., 2011; Gao et al., 2014, 2015) (owls and hummingbirds) but also what goes into frictional damping (Deng et al., 2023).

The results in **paper 3** and **paper 4** are not conclusive on the driving mechanisms for the twist of the feather. The results show that the behaviour of the feather is stable, with constant L/D that gives a predictable force output. Separating the L/D to its separate components we see that the lift force increases with twist, so it is possible that the increase in lift with sweep is more important than the drag penalty. Disregarding the drag penalty is also something we saw in **paper 1** and **paper 2** where the protruding shaft increased the drag. Suggesting the drag penalty is secondary to another function of the feather. With that said, the results in **paper 4**, suggest a link between sweep and drag, making it a possibility that the penalty in drag from the barbs and shaft is a mechanism that facilitates the backwards sweep.

7.2.6. Limitations

The larger feather model used in **paper 3** and **paper 4**, have the drawback that it is simplified and that it is fastened to a wall, but we do see that it behaves similar to the experimental feather. However, the results from **paper 4** are difficult to explain with the current model. It is possible that the actual movement of the barbs and barbules are necessary to fully model the feathers behaviour. Another aspect is the flight style; this is a limitation shared with the model for **paper 1** and **paper 2** as well. During flapping the angle of attack of the feathers and wings change (Klein Heerenbrink et al., 2015). It is therefore possible that some of the explanations of functionality, that have been difficult to explain, is rooted in flight style. The function has not been primarily selected for in the conditions that we have selected. Nevertheless, I argue that the results in this thesis is an initial step to understand the behaviour but there is still much work to be done before the passive behaviour of a feather is understood.

8. Final thoughts

The work in this thesis is a first step to understand the behaviour and the effect the 9th primary Jackdaw feather has on the air flow around it. It spans over the field of biology and engineering and try to combine separate knowledge into one. The results give a detailed description of the air flow around the mid part of the feather, it explores the feathers components (shaft, barbs and barbules) interaction with the air flow. It also explores the material properties and their effect on the behaviour of the feather, and finally how the morphology of the feather effects its behaviour.

The results offer potential explanations to why features on the feather, as the angle on the trailing vane, have evolved to have the angles we see today. It was shown that the aerodynamic efficiency was higher (**paper 2**) than for a layout that has lower trailing vane angels, as the evolutionary early birds had. So, even though the effective surface of the feather encapsulates all the rotating structures created by the feather component, they do influence the behaviour. Could there be a reason why a more effective surface hasn't been selected for. One explanation may be developmental constrains during the growth phase that hinders a simpler way of creating the aerodynamic surface, **paper 2**. With the findings in **paper 3**, another explanation for the complex barb/barbule system was presented. The large deflection we see in feathers, may be highly dependent on the relative movement between the barb/barbules. Exchanging to a solid system and potentially adding more mass would negatively affect the efficiency and stability and also add to the cost of flight.

The overall results suggest that the feather behaviour and responses, favour stability and predictability. The results suggest that trade-offs between the different functions in the feather, such as aerodynamic and structural performance are present, for example the drag penalty from the shaft. Even though there are commonalities with other biological systems, such as the low variability in lift oscillation amplitude in dragonflies, other benefits, such as drag reducing features (sharks, dragonflies) are missing. Lastly, we suggested a possible passive pitch mechanism in **paper 1** and **paper 2**, which would work in combination with the inherent twist of the feather. This mechanism would keep the feather in an optimal angle of attack. However, in **paper 4**, the results did not support the previous argument. There was no straight forward explanation of the twist from the aerodynamic perspective, and the twists may have functionalities that are still unknown.

As the complexities of the feather and its behaviour gradually came into light, from the inner structures of the shaft and barbs, the interaction between the barbs and barbules and the passive deflection in multiple directions at once. It became apparent that many aspects surrounding the feather remain unknown. Especially how the different feather component work together, their material properties and the best approach to model them. At the stage where I leave my thesis, the future possibilities appear endless. I argue that depending on your scope for your research, three different main avenues can be pursued, always keeping in mind the bigger picture. The main three approaches that I suggest is, first, continue and expand on the more detailed type of model presented **in paper 1** and **paper 2**. For example, a smaller highly detailed model at more locations along the feather could answer the different effects the tapering shaft has on the air flow. Continue to explore the effect the relative position of the components has on the flow behaviour, as in **paper 2**. It is also possible to change to model to include features we removed, such as how the barbule plane was modelled, add porosity close to the shaft or refine the approximation of the barbule representation. Second, explore the material and how to model it best. The material modelling was challenging both because there was a lack of data to support the material properties but also how the material was best modelled. Therefore, measuring all the aspects of the material and the behaviour of the feather under different conditions is a possibility. After, or in parallel, explore the setup of the mechanical modelling and/or the balance in the material properties. The results from **paper 3** and **paper 4**, suggest that the movement of the feather depends on the relative movement of the barbs and barbules and a model that reflects that would be interesting. Third, explore the behaviour of the feather and flow and morphologies on a larger model. The model used for **paper 3** and **paper 4** have its drawbacks, even so, it still shows similar behaviour as the experimental feather and can be used to gain more knowledge about the behaviour. However, another possibility is to increase the degrees of freedom, by no longer having it attached to the wall mid-point. Investigating the entire feather, the entire feather with added constraints or a feather attached to a wing could be a first step into a setup with less of the drawback seen. Another step could be to have several feathers, in a more slot like configuration to see the feathers full potential, even though there is a lot of work for it to be completed.

9. Thank you

I would like to thank my main supervisor Christoffer for all you have done; your support has been never ending. Your ability to put something into context and see beyond the immediate findings is inspiring.

My co-supervisors Johan and Kent, you have always been encouraging and guided me through the seemingly never-ending winding paths of modelling. Always finding new ways where I could not.

To all the people, present and past, connected to the Animal flight lab, Anders, Christoffer, Per, Gabriel, Linus, Pablo, Eric, Sonja, Daniele, Victor and Erica.

The institution of biology, you have embraced me as an engineer and made room for me. You have shown me a different way viewing the world and how to do thing. You have opened my eyes to the vastness that is biology.

To all how have helped me on the way with small and larger problem, or just a pep talk.

To everyone at Hand craft Thursdays, a lovely group of people to share one of my favourite hobbies. Once a week to clear my head and have a mini break from the tasks at hand. We have created some amazing things.

Thank you for my family, your never-ending support is life giving.

Finally, my wonderful, beloved husband Thomas. The one how always listens and cheers me on. I cherish every moment we have together, and our family. There are not enough words to express how thankful I am to have you in my life.

10. References

Ajanic, E., Paolini, A., Coster, C., Floreano, D., & Johansson, C. (2023). Robotic Avian Wing Explains Aerodynamic Advantages of Wing Folding and Stroke Tilting in Flapping Flight. *Advanced Intelligent Systems*, *5*(2), 2200148. https://doi.org/10.1002/aisy.202200148

Alenius, F., Revstedt, J., & Johansson, L. C. (2026). Feather aerodynamics suggest importance of lift and flow predictability over drag minimization. *Scientific Reports*, *16*(1), 8380. https://doi.org/10.1038/s41598-026-41064-7

Bachmann, T., Emmerlich, J., Baumgartner, W., Schneider, J. M., & Wagner, H. (2012). Flexural stiffness of feather shafts: Geometry rules over material properties. *Journal of Experimental Biology*, *215*(3), 405–415. https://doi.org/10.1242/jeb.059451

Badrya, C., Govindarajan, B., & Chopra, I. (2018). Basic Understanding of Unsteady Airfoil Aerodynamics at Low Reynolds Numbers. In *2018 AIAA Aerospace Sciences Meeting*. American Institute of Aeronautics and Astronautics. https://doi.org/10.2514/6.2018-2061

Bechert, D. W., Bruse, M., Hage, W., Hoeven, J. G. T. V. D., & Hoppe, G. (1997). Experiments on drag-reducing surfaces and their optimization with an adjustable geometry. *Journal of Fluid Mechanics*, *338*, 59–87. https://doi.org/10.1017/S0022112096004673

Berg, C. V. D., & Rayner, J. M. V. (1995). The Moment of Inertia of Bird Wings and the Inertial Power Requirement for Flapping Flight. *Journal of Experimental Biology*, *198*(8), 1655–1664. https://doi.org/10.1242/jeb.198.8.1655

Bonser, R., & Purslow, P. (1995). The Young's modulus of feather keratin. *Journal of Experimental Biology*, *198*(4), 1029–1033. https://doi.org/10.1242/jeb.198.4.1029

Bouard, F., Jardin, T., & David, L. (2024). Hovering flapping wings with dynamic twist. *Physics of Fluids*, *36*(11), 111910. https://doi.org/10.1063/5.0234656

Butler, M., & Johnson, A. S. (2004). Are melanized feather barbs stronger? *Journal of Experimental Biology*, *207*(2), 285–293. https://doi.org/10.1242/jeb.00746

Cameron, G. J., Wess, T. J., & Bonser, R. H. C. (2003). Young's modulus varies with differential orientation of keratin in feathers. *Journal of Structural Biology*, *143*(2), 118–123. https://doi.org/10.1016/S1047-8477(03)00142-4

Carruthers, A. C., Thomas, A. L. R., & Taylor, G. K. (2007). Automatic aeroelastic devices in the wings of a steppe eagle Aquila nipalensis. *Journal of Experimental Biology*, *210*(23), 4136–4149. https://doi.org/10.1242/jeb.011197

Chang, J., Zhang, Q., He, L., & Zhou, Y. (2022). Shedding vortex characteristics analysis of NACA 0012 airfoil at low Reynolds numbers. *Energy Reports, 2021 International Conference on New Energy and Power Engineering*, *8*, 156–174. https://doi.org/10.1016/j.egyr.2022.01.149

Chang, W.-L., Wu, H., Chiu, Y.-K., Wang, S., Jiang, T.-X., Luo, Z.-L., Lin, Y.-C., Li, A., Hsu, J.-T., Huang, H.-L., Gu, H.-J., Lin, T.-Y., Yang, S.-M., Lee, T.-T., Lai, Y.-C., Lei, M., Shie, M.-Y., Yao, C.-T., Chen, Y.-W., … Chuong, C.-M. (2019). The Making of a Flight Feather: Bio-architectural Principles and Adaptation. *Cell*, *179*(6), 1409-1423.e17. https://doi.org/10.1016/j.cell.2019.11.008

Chen, Z. J., Qin, N., & Nowakowski, A. F. (2013). Three-Dimensional Laminar-Separation Bubble on a Cambered Thin Wing at Low Reynolds Numbers. *Journal of Aircraft*, *50*(1), 152–163. https://doi.org/10.2514/1.C031829

Clark, C. J., Elias, D. O., & Prum, R. O. (2011). Aeroelastic Flutter Produces Hummingbird Feather Songs. *Science*, *333*(6048), 1430–1433. https://doi.org/10.1126/science.1205222

Clark, C. J., & Prum, R. O. (2015). Aeroelastic flutter of feathers, flight and the evolution of non-vocal communication in birds. *Journal of Experimental Biology*, *218*(21), 3520–3527. https://doi.org/10.1242/jeb.126458

Clyne, T. W., & Hull, D. (2019). *An Introduction to Composite Materials*. Cambridge University Press.

Dean, B., & Bhushan, B. (2010). Shark-skin surfaces for fluid-drag reduction in turbulent flow: A review. *Philosophical Transactions of the Royal Society A: Mathematical, Physical and Engineering Sciences*, *368*(1929), 4775–4806. https://doi.org/10.1098/rsta.2010.0201

Deng, K., Kovalev, A., Rajabi, H., Schaber, C. F., Dai, Z. D., & Gorb, S. N. (2021). The damping properties of the foam-filled shaft of primary feathers of the pigeon Columba livia. *The Science of Nature*, *109*(1), 1. https://doi.org/10.1007/s00114-021-01773-7

Deng, K., Schaber, C. F., Kovalev, A., Rajabi, H., Dai, Z. D., & Gorb, S. N. (2023). Aerodynamic vs. Frictional damping in primary flight feathers of the pigeon Columba livia. *Applied Physics A*, *129*(2), 121. https://doi.org/10.1007/s00339-023-06395-6

Dowell, E. H. (Ed.). (2022). *A Modern Course in Aeroelasticity* (Vol. 264). Springer International Publishing. https://doi.org/10.1007/978-3-030-74236-2

Eder, H., Fiedler, W., & Pascoe, X. (2011). Air-permeable hole-pattern and nose-droop control improve aerodynamic performance of primary feathers. *Journal of Comparative Physiology A*, *197*(1), 109–117. https://doi.org/10.1007/s00359-010-0592-7

Ennos, A. R., Hickson, J. R. E., & Roberts, A. (1995). Functional morphology of the vanes of the fliht feathers of the pegeon cloumba livia. *The Journal of Experimental Biology*, *198*, 1219–1228.

Feo, T. J., Field, D. J., & Prum, R. O. (2015). Barb geometry of asymmetrical feathers reveals a transitional morphology in the evolution of avian flight. *Proceedings of the Royal Society B: Biological Sciences*, *282*(1803), 20142864. https://doi.org/10.1098/rspb.2014.2864

Feo, T. J., & Prum, R. O. (2014). Theoretical morphology and development of flight feather vane asymmetry with experimental tests in parrots. *Journal of Experimental Zoology Part B: Molecular and Developmental Evolution*, *322*(4), 240–255. https://doi.org/10.1002/jez.b.22573

Feo, T. J., Simon, E., & Prum, R. O. (2016). Theory of the development of curved barbs and their effects on feather morphology. *Journal of Morphology*, *277*(8), 995–1013. https://doi.org/10.1002/jmor.20552

Foth, C., Tischlinger, H., & Rauhut, O. W. M. (2014). New specimen of Archaeopteryx provides insights into the evolution of pennaceous feathers. *Nature*, *511*(7507), Article 7507. https://doi.org/10.1038/nature13467

Fukami, K., Smith, L., & Taira, K. (2025). Extreme vortex-gust airfoil interactions at Reynolds number 5000. *Physical Review Fluids*, *10*(8), 084703. https://doi.org/10.1103/vcbd-tvz1

Gamble, L. L., Harvey, C., & Inman, D. J. (2020). Load alleviation of feather-inspired compliant airfoils for instantaneous flow control. *Bioinspiration & Biomimetics*, *15*(5), 056010. https://doi.org/10.1088/1748-3190/ab9b6f

Gao, J., Chu, J., Guan, L., Shang, H., & Lei, Z. (2014). Viscoelastic Characterization of Long-Eared Owl Flight Feather Shaft and the Damping Ability Analysis. *Shock and Vibration*, *2014*, e709367. https://doi.org/10.1155/2014/709367

Gao, J., Chu, J., Shang, H., & Guan, L. (2015). Vibration attenuation performance of long-eared owl plumage. *Bioinspired, Biomimetic and Nanobiomaterials*, *4*(3), 187–198. https://doi.org/10.1680/jbibn.15.00003

Gasiorek, J. M. K., Jack, L., Douglas, J. F., & Swaffield, J. (2006). *Fluid Mechanics* (J. F. Douglas, Ed.; 5th edition). Pearson College Div.

Greenwold, M. J., Bao, W., Jarvis, E. D., Hu, H., Li, C., Gilbert, M. T. P., Zhang, G., & Sawyer, R. H. (2014). Dynamic evolution of the alpha (α) and beta (β) keratins has accompanied integument diversification and the adaptation of birds into novel lifestyles. *BMC Evolutionary Biology*, *14*(1), 249. https://doi.org/10.1186/s12862-014-0249-1

Hamman, C. W., Klewicki, J. C., & Kirby, R. M. (2008). On the Lamb vector divergence in Navier–Stokes flows. *Journal of Fluid Mechanics*, *610*, 261–284. https://doi.org/10.1017/S0022112008002760

Harvey, C., de Croon, G., Taylor, G. K., & Bomphrey, R. J. (2023). Lessons from natural flight for aviation: Then, now and tomorrow. *Journal of Experimental Biology*, *226*(Suppl_1), jeb245409. https://doi.org/10.1242/jeb.245409

Hendrickx-Rodriguez, S., & Lentink, D. (2025). The feather's multi-functional structure across nano to macro scales inspires hierarchical design. *Journal of The Royal Society Interface*, *22*(225), 20240776. https://doi.org/10.1098/rsif.2024.0776

Introduction to wind turbine blade design. (2023). In *Advances in Wind Turbine Blade Design and Materials* (pp. 3–53). Woodhead Publishing. https://doi.org/10.1016/B978-0-08-103007-3.00009-4

Kesel, A. B. (2000). Aerodynamic characteristics of dragonfly wing sections compared with technical aerofoils. *Journal of Experimental Biology*, *203*(20), 3125–3135. https://doi.org/10.1242/jeb.203.20.3125

Kiat, Y., & O'Connor, J. K. (2024). Functional constraints on the number and shape of flight feathers. *Proceedings of the National Academy of Sciences*, *121*(8), e2306639121. https://doi.org/10.1073/pnas.2306639121

Klein Heerenbrink, M., Johansson, L. C., & Hedenström, A. (2015). Power of the wingbeat: Modelling the effects of flapping wings in vertebrate flight. *Proceedings of the Royal Society A: Mathematical, Physical and Engineering Sciences*, *471*(2177), 20140952. https://doi.org/10.1098/rspa.2014.0952

KleinHeerenbrink, M., Johansson, L. C., & Hedenström, A. (2017). Multi-cored vortices support function of slotted wing tips of birds in gliding and flapping flight. *Journal of The Royal Society Interface*, *14*(130), 20170099. https://doi.org/10.1098/rsif.2017.0099

KleinHeerenbrink, M., Warfvinge, K., & Hedenström, A. (2016). Wake analysis of aerodynamic components for the glide envelope of a jackdaw (Corvus monedula). *Journal of Experimental Biology*, *219*(10), 1572–1581. https://doi.org/10.1242/jeb.132480

Klose, B. F., Spedding, G. R., & Jacobs, G. B. (2021). *Direct numerical simulation of cambered airfoil aerodynamics at Re = 20,000* (arXiv:2108.04910). arXiv. https://doi.org/10.48550/arXiv.2108.04910

Klose, B. F., Spedding, G. R., & Jacobs, G. B. (2025). Flow separation, instability and transition to turbulence on a cambered airfoil at Reynolds number 20 000. *Journal of Fluid Mechanics*, *1009*, A9. https://doi.org/10.1017/jfm.2025.212

Kovalev, A., Filippov, A. E., & Gorb, S. N. (2014). Unzipping bird feathers. *Journal of The Royal Society Interface*, *11*(92), 20130988. https://doi.org/10.1098/rsif.2013.0988

Lentink, D., & Kat, R. de. (2014). Gliding Swifts Attain Laminar Flow over Rough Wings. *PLOS ONE*, *9*(6), e99901. https://doi.org/10.1371/journal.pone.0099901

Levy, D.-E., & Seifert, A. (2009). Simplified dragonfly airfoil aerodynamics at Reynolds numbers below 8000. *Physics of Fluids*, *21*(7), 071901. https://doi.org/10.1063/1.3166867

Li, Q., Shen, H., Han, Q., Ji, A., Dai, Z., & Gorb, S. N. (2022). Effects of Morphological Integrity of Secondary Feather on Their Drag Reduction in Pigeons. *Journal of Bionic Engineering*, *19*(5), 1422–1438. https://doi.org/10.1007/s42235-022-00203-2

Lingham-Soliar, T. (2014). Feather structure, biomechanics and biomimetics: The incredible lightness of being. *Journal of Ornithology*, *155*(2), 323–336. https://doi.org/10.1007/s10336-013-1038-0

Lingham-Soliar, T., Bonser, R. H. C., & Wesley-Smith, J. (2009). Selective biodegradation of keratin matrix in feather rachis reveals classic bioengineering. *Proceedings of the Royal Society B: Biological Sciences*, *277*(1685), 1161–1168. https://doi.org/10.1098/rspb.2009.1980

Lingham-Soliar, T., & Murugan, N. (2013). A New Helical Crossed-Fibre Structure of β-Keratin in Flight Feathers and Its Biomechanical Implications. *PLOS ONE*, *8*(6), e65849. https://doi.org/10.1371/journal.pone.0065849

Liu, D., Song, B., Yang, W., Yang, X., Xue, D., & Lang, X. (2021). A Brief Review on Aerodynamic Performance of Wingtip Slots and Research Prospect. *Journal of Bionic Engineering*, *18*(6), 1255–1279. https://doi.org/10.1007/s42235-021-00116-6

Liu, G. R., & Quek, S. S. (2013). *The Finite Element Method: A Practical Course*. Butterworth-Heinemann. https://doi.org/10.1016/C2012-0-00779-X

Liu, H., Wang, S., & Liu, T. (2024). Vortices and Forces in Biological Flight: Insects, Birds, and Bats. *Annual Review of Fluid Mechanics*, *56*(Volume 56, 2024), 147–170. https://doi.org/10.1146/annurev-fluid-120821-032304

Lucas, A. M., & Stettenheim, P. R. (1972). *Avian anatomy Integument Part 1 and 2*.

McArthur, J. (2008). *Aerodynamics of wings at low reynolds numbers: Boundary layer separation and reattachment*. University of Southern California.

Murayama, Y., Nakata, T., & Liu, H. (2021). Flexible Flaps Inspired by Avian Feathers Can Enhance Aerodynamic Robustness in low Reynolds Number Airfoils. *Frontiers in Bioengineering and Biotechnology*, *9*. https://doi.org/10.3389/fbioe.2021.612182

Norberg, R. Å. (1985). *Function of Vane Asymmetry and Shaft Curvature in Bird Flight Feathers; Inference of Flight Abilit of Archaeopteryx*. 16.

Norberg, U. M. (1990). *Vertebrate flight*. Springer.

Oeffner, J., & Lauder, G. V. (2012). The hydrodynamic function of shark skin and two biomimetic applications. *Journal of Experimental Biology*, *215*(5), 785–795. https://doi.org/10.1242/jeb.063040

Okamoto, M., Yasuda, K., & Azuma, A. (1996). Aerodynamic characteristics of the wings and body of a dragonfly. *Journal of Experimental Biology*, *199*(2), 281–294. https://doi.org/10.1242/jeb.199.2.281

Oorschot, B. K. van, Choroszucha, R., & Tobalske, B. W. (2020). Passive aeroelastic deflection of avian primary feathers. *Bioinspiration & Biomimetics*, *15*(5), 056008. https://doi.org/10.1088/1748-3190/ab97fd

Pandi, J. S. S., & Mittal, S. (2025). Twisted finite wing at low Reynolds number: Cellular vortex shedding, wing-tip vortex and aerodynamic performance. *Journal of Fluid Mechanics*, *1002*, A28. https://doi.org/10.1017/jfm.2024.1152

Pennycuick, C. (2008). *Modelling the Flying Bird* (Vol. 5). Elsevier. https://doi.org/10.1016/S1875-306X(08)00017-8

Pennycuick, C., Alerstam, T., & HedenstrÖM, A. (1997). A new low-turbulence wind tunnel for bird flight experiments at Lund University, Sweden. *The Journal of Experimental Biology*, *200*(Pt 10), 1441–1449. https://doi.org/10.1242/jeb.200.10.1441

Polo, V., & Carrascal, L. M. (n.d.). PTILOCHRONOLOGY AND FLUCTUATING ASYMMETRY IN TAIL AND WING FEATHERS OF COAL TITS. *Ardeola*. Retrieved https://share.google/2gXGstZIlyuHXLFgS

Prum, R. O. (1999). Development and evolutionary origin of feathers. *Journal of Experimental Zoology*, *285*(4), 291–306. https://doi.org/10.1002/(SICI)1097-010X(19991215)285:4%3C291::AID-JEZ1%3E3.0.CO;2-9

Purslow, P. P., & Vincent, J. F. V. (n.d.). *MECHANICAL PROPERTIES OF PRIMARY FEATHERS FROM THE PIGEON*.

Sauvageat, E. (2016). *Infoscience—EPFL Institutional Repository Viewer*. https://infoscience.epfl.ch/entities/publication/d6da3621-0d3e-45a8-ae75-b53ada6d4b02

Sawyer, R. H., Glenn, T., French, J. O., Mays, B., Shames, R. B., George L. Barnes, J., Rhodes, W., & Ishikawa, Y. (2000). The Expression of Beta (β) Keratins in the Epidermal Appendages of Reptiles and Birds1. *American Zoologist*, *40*(4), 530–539. https://doi.org/10.1668/0003-1569(2000)040%5B0530:TEOBKI%5D2.0.CO;2

Schmitz, A., Ponitz, B., Brücker, C., Schmitz, H., Herweg, J., & Bleckmann, H. (2015). Morphological properties of the last primaries, the tail feathers, and the alulae of Accipiter nisus, Columba livia, Falco peregrinus, and Falco tinnunculus. *Journal of Morphology*, *276*(1), 33–46. https://doi.org/10.1002/jmor.20317

Spedding, G. R., Hedenström, A. H., McArthur, J., & Rosén, M. (2008). The implications of low-speed fixed-wing aerofoil measurements on the analysis and performance of flapping bird wings. *Journal of Experimental Biology*, *211*(2), 215–223. https://doi.org/10.1242/jeb.007823

Sullivan, T. N., Meyers, M. A., & Arzt, E. (2019). Scaling of bird wings and feathers for efficient flight. *Science Advances*, *5*(1), eaat4269. https://doi.org/10.1126/sciadv.aat4269

Sullivan, T. N., Pissarenko, A., Herrera, S. A., Kisailus, D., Lubarda, V. A., & Meyers, M. A. (2016). A lightweight, biological structure with tailored stiffness: The feather vane. *Acta Biomaterialia*, *41*, 27–39. https://doi.org/10.1016/j.actbio.2016.05.022

Sullivan, T. N., Wang, B., Espinosa, H. D., & Meyers, M. A. (2017). Extreme lightweight structures: Avian feathers and bones. *Materials Today*, *20*(7), 377–391. https://doi.org/10.1016/j.mattod.2017.02.004

Tank, J., Smith, L., & Spedding, G. R. (2017). On the possibility (or lack thereof) of agreement between experiment and computation of flows over wings at moderate Reynolds number. *Interface Focus*, *7*(1), 20160076. https://doi.org/10.1098/rsfs.2016.0076

Terrill, R. S., & Shultz, A. J. (2023). Feather function and the evolution of birds. *Biological Reviews*, *98*(2), 540–566. https://doi.org/10.1111/brv.12918

van Bokhorst, E., de Kat, R., Elsinga, G. E., & Lentink, D. (2015). Feather roughness reduces flow separation during low Reynolds number glides of swifts. *Journal of Experimental Biology*, *218*(20), 3179–3191. https://doi.org/10.1242/jeb.121426

Vargas, A., Mittal, R., & Dong, H. (2008). A computational study of the aerodynamic performance of a dragonfly wing section in gliding flight. *Bioinspiration & Biomimetics*, *3*(2), 026004. https://doi.org/10.1088/1748-3182/3/2/026004

Versteeg, H. K., & Malalasekera, W. (n.d.). *An introduction to computational fluid dynamics. The finite volume method* (second edition, Vol. 2007). Pearson Education Limited.

Wakeling, J. M., & Ellington, C. P. (1997). Dragonfly Flight: I. Gliding Flight and Steady-State Aerodynamic Forces. *Journal of Experimental Biology*, *200*(3), 543–556. https://doi.org/10.1242/jeb.200.3.543

Walker, S. M., Thomas, A. L. R., & Taylor, G. K. (2009). Photogrammetric reconstruction of high-resolution surface topographies and deformable wing kinematics of tethered locusts and free-flying hoverflies. *Journal of the Royal Society, Interface*, *6*(33), 351–366. https://doi.org/10.1098/rsif.2008.0245

Wang, B., & Meyers, M. A. (2017). Light Like a Feather: A Fibrous Natural Composite with a Shape Changing from Round to Square. *Advanced Science*, *4*(3), 1600360. https://doi.org/10.1002/advs.201600360

Wang, X., Tang, H. K., & Clarke, J. A. (2019). Flight, symmetry and barb angle evolution in the feathers of birds and other dinosaurs. *Biology Letters*, *15*(12), 20190622. https://doi.org/10.1098/rsbl.2019.0622

Weiss, I. M., & Kirchner, H. O. K. (2010). The peacock's train (Pavo cristatus and Pavo cristatus mut. Alba) I. structure, mechanics, and chemistry of the tail feather coverts. *Journal of Experimental Zoology Part A: Ecological Genetics and Physiology*, *313A*(10), 690–703. https://doi.org/10.1002/jez.641

Winslow, J., Otsuka, H., Govindarajan, B., & Chopra, I. (2018). Basic Understanding of Airfoil Characteristics at Low Reynolds Numbers (104–105). *Journal of Aircraft*, *55*(3), 1050–1061. https://doi.org/10.2514/1.C034415

Wiswell, H., & Wissa, A. (2026a). Aerodynamic Mechanisms and Flow Physics of Bioinspired Slotted Wingtips. *Integrative and Comparative Biology*, *66*, icag036. https://doi.org/10.1093/icb/icag036

Wiswell, H., & Wissa, A. (2026b). Aerodynamic Mechanisms and Flow Physics of Bioinspired Slotted Wingtips. *Integrative and Comparative Biology*, icag036. https://doi.org/10.1093/icb/icag036

Xu, X., Zhou, Z., Dudley, R., MacKem, S., Chuong, C.-M., Erickson, G. M., & Varricchio, D. J. (2014). An integrative approach to understanding bird origins. *Science*, *346*(6215). Scopus. https://doi.org/10.1126/science.1253293